Deep-Sea Research I 88 (2014) 47–62

Contents lists available at ScienceDirect

Deep-Sea Research I

journal homepage: www.elsevier.com/locate/dsri

Phytoplankton community structures in shelf and oceanic waters off southeast Brazil (20°–25°S), as determined by pigment signatures

Silvana V. Rodrigues [a,*,1], Marcelo M. Marinho [b,1], Cássia C. Cubas Jonck [a], Eline S. Gonçalves [a], Vinnicius F. Brant [a], Rodolfo Paranhos [c], Maria Patrícia Curbelo [d], Ana Paula Falcão [d]

[a] Instituto de Química, Universidade Federal Fluminense, Outeiro de S. João Batista S/N, Niterói, RJ, Brazil
[b] Laboratório de Ecologia e Fisiologia do Fitoplâncton, Departamento de Biologia Vegetal, Universidade do Estado do Rio de Janeiro, Rua São Francisco Xavier 524—PHLC sala 511a, Rio de Janeiro, RJ, Brazil
[c] Instituto de Biologia, Universidade Federal do Rio de Janeiro, Av. Prof. Rodolpho Rocco 211, CCS, bl. A, sala A1-071, Ilha do Fundão, Rio de Janeiro, RJ, Brazil
[d] Petróleo Brasileiro S.A.—PETROBRAS, CENPES, Av. Horácio Macedo 950, Cidade Universitária, Rio de Janeiro, RJ, Brazil

ARTICLE INFO

Article history:
Received 17 June 2013
Received in revised form
11 February 2014
Accepted 19 March 2014
Available online 31 March 2014

Keywords:
Photosynthetic pigments
HPLC
CHEMTAX
Chemotaxonomy
Campos Basin

ABSTRACT

The influences of the hydrological features and environmental conditions in the phytoplankton community found in the Campos Basin area in the Atlantic Ocean (20° to 25°S; 42° to 38°W) were studied using HPLC/CHEMTAX pigment analysis. Samples were collected at 72 stations distributed along the 25–3000 m isobaths at two depths during two seasonal periods (rainy and dry). Seven taxonomic groups of phytoplankton were detected (diatoms, dinoflagellates, prasinophytes, cryptophytes, haptophytes, pelagophytes and cyanobacteria). Redundancy analysis showed that the spatial and temporal patterns observed in the distribution of the phytoplanktonic groups were primarily related to variations in the availability of light and nutrients. Nutrient variations were caused by South Atlantic Central Water seasonal intrusions over the continental shelf region. Cyanobacteria predominated in the rainy season, while diatoms, Haptophyceae and Prasinophyceae, were associated with higher nutrient availability in the dry season. In the inner shelf region, diatoms dominated and were associated with increased conditions of turbulence and nutrient availability. Haptophytes and prasinophytes were predominant on the outer shelf and shelf-break regions associated with high nutrient concentrations and availability of light. *Prochlorococcus* was related to oceanic waters (in both dry and rainy periods) or to low nutrient/strongly stratified shelf waters (rainy period). In contrast, *Synechococcus* was widely distributed in both the shelf and oceanic regions. Variation in the quality of light between coastal and oceanic waters was probably responsible for the distributions observed. Through HPLC/CHEMTAX pigment analysis we have developed a detailed picture of the influence of hydrological regime on the dynamics of the phytoplankton community in an under-studied shelf/ocean system in the tropical southern Atlantic Ocean.

1. Introduction

Estimating the composition and biomass of phytoplankton is of great importance for understanding the structure and dynamics of pelagic ecosystems (Ediger et al., 2006). As the major primary producers in many aquatic systems and the basis of nearly all food webs in aquatic ecosystems (Arrigo, 2005), phytoplankton are essential for marine ecological and biogeochemical processes.

In tropical marine waters, the phytoplankton communities consist of autotrophic, heterotrophic and mixotrophic organisms of variable size. While diatoms dominate in terms of species diversity in coastal and shelf regions, their relative importance is gradually reduced toward the open ocean, where the contribution of dinoflagellates increases significantly (Fernandes and Brandini, 2004). On continental shelves, the contribution of nanoplanktonic haptophytes is also important (Simon et al., 2009). In open seas, picoplankton (primarily consisting of cyanobacteria and small eukaryotes) dominate both the photosynthetic biomass and production (Vaulot et al., 2008; Simon et al., 2009).

The tropical and subtropical waters of the Atlantic Ocean along the Brazilian, Uruguayan and Argentinean coasts are influenced by a variety of hydrographic processes, which promote great diversity

* Correspondence to: Departamento de Química Analítica, Instituto de Química, 23 Universidade Federal Fluminense, Outeiro de S. João Batista, S/N, Centro, 24.020-141 Niterói - 24 RJ - Brasil. Tel.: +55 21 26292140; fax: +55 21 26292143.
E-mail address: silvana@vm.uff.br (S.V. Rodrigues).
[1] Both authors contributed equally to this work.

http://dx.doi.org/10.1016/j.dsr.2014.03.006
0967-0637/

in the biological systems and result in several biogeographical provinces, from the oligotrophic waters of the South Atlantic gyre to the highly productive coastal waters at the La Plata river (35°S) and the Patos Lagoon (32°S) fronts (Gonzalez-Silvera et al., 2004).

Microphytoplankton in the Central Region of the Brazilian shelf waters (22–19°S) are typical of oligotrophic tropical oceans, with low density ($<10^3$ cell L^{-1}) and high diversity and dominance of thermophile species and heterotrophic dinoflagellates (Tenenbaum et al., 2006). Diatoms and flagellated cells of nano- and microplankton belonging to the groups Dynophyceae, Haptophyceae, Cryptophyceae, Prasinophyceae and Chlorophyceae are dominant among the taxonomic groups present on the Brazilian Shelf (Fernandes and Brandini, 2004). Blooms of the filamentous cyanobacteria *Trichodesmium* are also common (Sato et al., 1963; Brandini, 1988; Gianesella-Galvão et al., 1995). Although the phytoplankton composition has been determined in the Cabo Frio region (23°S) in terms of the size-fractioned chlorophyll *a* biomass (Guenther et al., 2008), and the total pico-, nano- and microplankton biomass in the region between Cabo de São Tomé (22°S) and Salvador (13°S) was analyzed using epifluorescence microscopy (Tenenbaum et al., 2006), a comprehensive assessment encompassing the full phytoplankton size range is still lacking.

Assessments performed via inverted microscopy can underestimate the biomass of small phytoplankton and may not always distinguish photoautotrophic from heterotrophic cells (Seoane et al., 2011). Furthermore, nanoplanktonic flagellates can be difficult to identify using this technique, as is the case for haptophytes of the genus *Phaeocystis* sp., which display a worldwide distribution and occur in highly diverse marine systems (Schoemann et al., 2005). The development of electron microscopy has allowed unambiguous determination of picoplanktonic species, such as *Bathycoccus prasinos* or *Imantonia rotunda*, and the importance of some groups has been established as a result (Vaulot et al., 2008). However, electron microscopy is a difficult and time-consuming technique. Cellular flow cytometry analysis allows determination of the biomass of the three main picophytoplanktonic (<2–3 μm) groups present in open oceans: cyanobacteria of the *Prochlorococcus* and *Synechococcus* genera and eukaryotes belonging to diverse taxa (Grob et al., 2007). However, in many cases, scattering and fluorescence properties are not sufficient to discriminate picoeukaryote taxa, with the exception of cryptophytes (Vaulot et al., 2008). In recent years, the composition of marine picoeukaryote communities has been intensively investigated using molecular approaches, but adequate assessment of the photosynthetic fraction involves very sophisticated methods based on flow cytometry sorting, followed by the construction of 18S rRNA gene clone libraries (Shi et al., 2009). These methods cannot yet be employed on a routine basis for measuring the full size range of phytoplankton (Schlüter et al., 2011).

The presence of photosynthetic pigments does not depend on phytoplankton size and can be analyzed via High performance liquid chromatography/UV–vis absorption Diode array detection (HPLC/DAD), which is a widely applied technique. Some pigments unambiguously identify a certain class or a genus (e.g., prasinoxanthin in some prasinophytes), while others are common to multiple classes (e.g., fucoxanthin). Therefore, although mathematical methods have been developed to express the contribution of taxonomic groups to Chl *a* (Gieskes et al., 1988; Letelier et al., 1993; Obayashi et al., 2001), reconstruction of the phytoplankton composition based on pigment concentrations is not straightforward. Mackey et al. (1997) proposed a data-fitting technique for estimating the Chl *a* content of taxonomic groups using pigment data, the CHEMTAX program. It uses factor analysis and a steepest descent algorithm to find the best fit to the data based on suggested marker pigment/Chlorophyll a ratios for the phytoplankton groups to be determined. Detailed analysis of pigments from natural samples allows the identification of phytoplanktonic taxonomic groups and this approach has been used in many aquatic ecosystems including marine and freshwater habitats (Marinho and Rodrigues, 2003; Carreto et al., 2008; Wright et al., 2010; Gonçalves-Araujo et al., 2012). However, there have been few studies addressing phytoplankton pigments from the tropical South Atlantic, and, to our knowledge, no previous data are available in the region of the present study.

This study was conducted in the Campos Basin, located within the Brazil Shelf Large Marine Ecosystem. The water masses that comprise this region are the Coastal Water (CW), Tropical Water (TW) and the South Atlantic Central Water (SACW), the latter two of oceanic origin, transported by the Brazil Current. Coastal upwelling and intrusions of waters from the oceanic pycnocline (SACW) onto the continental shelf of southeast Brazil are phenomena controlled by various physical processes, which operate at multiple space and time scales (Palóczy et al., 2013). Our hypothesis is that the intrusions of SACW drive biological processes from the coastal to the oceanic region and the responses of biotic communities including the phytoplankton. HPLC/CHEMTAX analysis of pigments was used as a tool to bring insight into the structure of the phytoplankton assemblages, including phytoplankton taxa generally underestimated or overlooked by microscopy. In particular we addressed two questions: (1) How is this structure influenced by the hydrologic features of the region? (2) How do the assemblages correlate with the environmental conditions?

2. Methodology

2.1. Study area

This study was conducted in the Campos Basin region, located in the Atlantic Ocean (20° to 25°S; 42° to 38°W), adjacent to the southeastern coast of Brazil (Fig. 1). This region is located within two biogeographical provinces, one characterized by oligotrophic waters with coastal influence and the other by upwelling phenomena, located in Cabo Frio (Gonzalez-Silvera et al., 2004). The Campos Basin is divided between the eastern and southern portions of the Brazil Shelf Large Marine Ecosystem. Samples were collected at stations distributed along the 25, 50, 75, 150, 400, 1000, 1900 and 3000 m isobaths, along nine transects ranging from south to north (designated A–I), during two campaigns, one

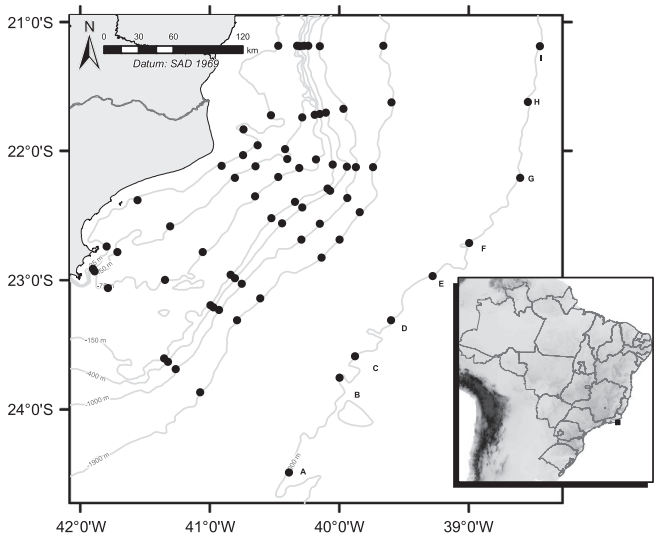

Fig. 1. Study Area: Transects (A–I), isobaths (25–3000 m). Black circles represent sampling stations.

of which was performed in the rainy season (between March 5th and April 13th, 2009) and the other in the dry season (between August 7th and September 16th, 2009). At each station, samples were collected from the sub-surface (1 m) and at a second depth defined for the 25, 50 and 75 m isobaths as the middle of the water column, or as the 20 °C isotherm (typical of the South Atlantic Central Water), when it was detected. For the stations at the isobaths of 150, 400, 1000, 1900 and 3000 m, it was the depth at which the water temperature was 0.5 °C below that at the surface, which typically corresponded to the depth of the upper mixed layer (Fig. 1). On the continental shelf, the second depth ranged from 10 to 56 m during the rainy season and from 11 to 53 m during the dry season. At the oceanic region, it varied from 18 to 60 m and from 17 to 130 m in the rainy and dry seasons, respectively.

2.2. Environmental data

The environmental data used in our analysis included physical (water temperature and salinity obtained by a CTD) and chemical (inorganic nutrients analyzed by standard oceanographic methods (Grasshoff et al., 1999)) variables. The euphotic zone (Z_{euf}) was estimated as 3 times the Secchi disk extinction depth (Cole, 1994). Detailed discussion about the hydrochemistry of the study area is presented elsewhere (Suzuki et al., in press).

2.3. HPLC analysis of pigments

Samples for the analysis of phytoplankton pigments were obtained by filtering 6 L of seawater through GF/F 47 mm membranes (Whatman, UK) under reduced light at a minimum pressure of 250 mmHg. The filters were immediately placed in cryovials and stored in liquid nitrogen until analysis. The pigments were extracted using the method described by Wright and Jeffrey (1997), with some modification: trans-beta-apo-8′-carotenal (Sigma Aldrich, USA), which is often used as an internal standard (Wright et al., 2010), was added immediately before the ultrasound-assisted extraction step (using a Bandelin Sonoplus probe, Berlin, Germany). The samples were then analyzed according to Van Heukelem and Thomas (2001), (Method 1), and Brotas and Plante-Cuny (2003), (Method 2), using a Thermo Accella model 600 chromatograph with a diode array detector (Thermo Scientific, USA) and a Bischoff Analysentechnik chromatograph (Leonberg, Germany) coupled to a SPD-M10A VP diode array detector (Shimadzu, Kyoto, Japan). In Method 1, the Eclipse C8 150 mm, 3 μm (Agilent, Technologies, Waldbronn, Germany) column used by Van Heukelem and Thomas (2001) was replaced with an ACE C8 150 mm, 3 μm column (Advanced Chromatography Technologies Ltd, UK), and the flow rate was changed to 1.2 mL min^{-1}. The use of an ACE C8 column was advantageous for improving the separation of the pairs chlorophyll b/divinyl-chlorophyll b and chlorophyll a/divinyl-chlorophyll a. However, the carotenoids 19′hexanoyloxifucoxanthin, prasinoxanthin and violaxanthin were coeluted, and β,ε- and β,β-carotene were not entirely resolved (Fig. 2a). Method 2 did not resolve the monovinyl/divinyl pairs of chlorophylls *a* and *b* (Fig. 2b). All samples were analyzed in parallel with Methods 1 and 2. The quality of the extraction was controlled by the recovery of trans-beta-apo-8′-carotenal (ApoCar) added in the extraction medium. ApoCar was not used as an internal standard, to avoid confusing the efficiency of the extraction of individual pigments from the cells with the recovery of the free added carotenoid. Furthermore, the fact that the extracts were analyzed by two parallel HPLC methods helped to verify whether there had been an extraction or an injection problem (i.e., if the area of ApoCar was low by only one method, an injection problem was detected). The pigment contents were quantified using standards for chlorophyll *c3* (Chl *c3*), chlorophyll *c2* (Chl *c2*),

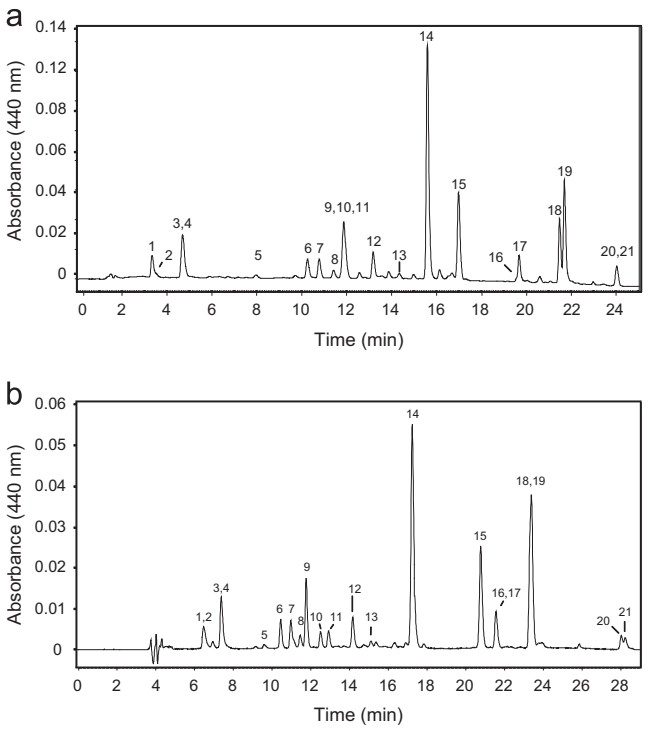

Fig. 2. Separation of pigments from sample B3, second depth, rainy period. Method: (a) modified from Van Heukelem and Thomas (2001); (b) Brotas and Plante-Cuny (2003). Pigments: 1—Chl *c3*, 2—MV Chl *c3*, 3—Chl *c2*, 4—Chl *c1*, 5—Per, 6—19′But, 7—Fuco, 8—Neo, 9—19′Hex, 10—Pras, 11—Viola, 12—Diadino, 13—Allo, 14—Zea, 15—I.S. (Trans-beta-Apo 8′-Carotenal), 16—DV Chl *b*, 17—Chl *b*, 18—DV Chl *a*, 19—Chl *a*, 20—β,ε-Car, 21—ββ-Car.

chlorophyll *b* (Chl *b*), divinyl-chlorophll *a* (DV Chl *a*), chlorophyll *a* (Chl *a*), peridinin (Per), 19′butanoyloxifucoxanthin (19′But), fucoxanthin (Fuco), 19′hexanoyloxifucoxanthin (19′Hex), zeaxanthin (Zea), lutein (Lut), prasinoxanthin (Pras), neoxanthin (Neox), violaxanthin (Viola), diadinoxanthin (Diad), diatoxanthin (Diat), alloxanthin (Allo), mixoxantophyll (Mixo), β,ε-carotene (β,ε-Car) and β,β-carotene (β,β-Car), obtained from DHI-Water and Environment (Hørsholm, Denmark). All of the pigments were quantified at 440 nm, except mixoxantophyll, which was analyzed at 503 nm. The application of the two methods enabled the quantification of 21 pigments, at detection limits between 0.1 and 2 μg m^{-3} (calculated according to Miller and Miller, 1988). Total chlorophyll *a* (TChl *a*) concentration, which was used as an indicator of phytoplankton biomass, was estimated as the sum of Chl *a* and DV Chl *a* concentrations in each sample.

Chl *a*, DV Chl *a*, Chl *b*, and DV Chl *b* concentrations were taken from HPLC Method 1 because Method 2 did not resolve the monovinyl/divinyl pairs. Mixo was quantified by Method 1, because of the higher sensitivity observed. 19′Hex, Pras and Viola were quantified by Method 2 because they were not resolved by Method 1. Per was also quantified by Method 2 because peak purity was higher than by Method 1. Since the average difference between the concentrations obtained from the two methods was 10–20%, concentrations of well resolved pigments could be taken from either of the methods. In the rainy period, Chl *c3*, Chl *c2*, 19′But, Fuco, Neo, Allo, and Mixo were also taken from Method 1; in the dry period only the mono/divinyl pairs were taken from Method 1.

2.4. Processing of pigment data—CHEMTAX analysis

The relative contributions of different phytoplankton groups to the observed chlorophyll *a* content was calculated for each

sampling station using CHEMTAX software, version 1.95 (Mackey et al., 1997). The following pigments were included in the matrices: Chl *c3*, Chl *c2*, Chl *b*, DV Chl *a*, Chl *a*, Per, 19′But, Fuco, 19′Hex, Zea, Lut, Pras, Neox, Viola, Allo and Mixo. The initial pigment ratios in the algal taxa used in the chemotaxonomic analysis were obtained from the literature (Carreto et al., 2008; Schlüter et al., 2011) because pigment ratios from local phytoplankton were not determined in the present study. Pigment ratios for diatoms were taken from Carreto et al. (2003). For *Synechococcus*, prasinoxanthin-containing prasinophytes (Pras 1), violaxanthin-containing prasinophytes (Pras 2), cryptophytes (Crypto), pelagophytes (Pelago) and dinoflagellates (Dino) the mean pigment ratios of unialgal cultures of *Synechococcus*, *Pycnococcus provasolii* (*Pras 1*), *Pyramimonas disomata* (*Pras 2*), *Rhodomonas salina* (*Crypto*), *Pelagococcus subviridis* (*Pelago*) and *Prorocentrum micans* (*Dino*), grown under different light intensities (Schlüter et al., 2000), were used. The only reference for pigment ratios of filamentous cyanobacteria were the *Trichodesmium* ratios found in Mackey et al. (1997). This study was also used for the pigment ratio of *Prochlorococcus* (Zea/DV Chl *a*). The inclusion of three types of haptophytes in the input matrix was based on the detected pigments, on previous findings in the south of Brazil (Bergesch et al., 2008) and on the high complexity of haptophytes, which have eight subgroups with different pigment profiles (Zapata et al., 2004); the respective pigment profiles were taken from the values obtained by Carreto et al. (2008) in the Southern Atlantic.

Samples collected for microplankton microscopic analysis were consistent with the constructed CHEMTAX input matrix: diatoms were mainly represented by *Chaetoceros, Rhizosolenia, Dactyliosolen, Leptocylindrus* and *Pseudo-nitzschia* in the rainy period and *Dactyliosolen* and *Guinardia* in the dry period; dinoflagellates consisted mainly of the genus *Prorocentrum* in the south of the Campos Basin in the rainy period and of unidentified tecate species in the shelf in both periods; filamentous cyanobacteria were important in the rainy period (Tenenbaum et al., in press).

For chemotaxonomic analysis, samples were divided in groups according to both the depth and spatial distribution observed for the pigments. In each campaign, four groups were defined: Group 1: samples collected at 1 m in the 25, 50 and 75 m isobaths; Group 2: samples collected at the second depth in the 25, 50 and 75 m isobaths (second depth); Group 3: samples collected at 1 m in the 150, 400, 1000, 1900, 3000 m isobaths; and Group 4: samples collected at the second depth in the 150, 400, 1000, 1900, 3000 m isobaths (second depth). The CHEMTAX analysis followed the procedure adopted by Wright et al. (2009): 60 ratio matrixes were generated by multiplying each cell of the initial ratio matrix by a randomly determined factor, F, where $F=1+S\times(R\ ¡\ 0.5)$; S is a scaling factor (normally 0.7); and R is a random number between 0 and 1. Each of the 60 ratio tables was employed as the starting point for a CHEMTAX optimization, resulting in 60 solutions. To generate the final results, the six best solutions (those with the smallest residuals) were averaged. The biomasses of taxonomic groups were expressed in terms of their Chl *a* content, except *Prochlorococcus*, which was expressed in terms of the concentration of DV Chl *a*.

2.5. Statistical analysis

To verify the similarities along transects (latitudinal pattern), a permutational multivariate analysis of variance (PERMANOVA) for models with multiple factors (Anderson, 2001) was performed. We analyzed two factors (transects and isobaths), and the pigment values obtained at the two depths were considered as replicates. The Bray–Curtis distance was chosen as a measure of dissimilarity for all analyses, and 9999 permutations were run for each analysis for tests with a significance level of 0.05. In the case of a significant result, affinity patterns were identified through *a posteriori* tests using 999 permutations. Similarities between the isobaths (bathymetric profile) and between the depths (vertical profile) sampled were verified through analysis of similarity (ANOSIM) and via a nonparametric test of significance (applying a Bonferroni correction to the resulting p values) in similarity matrices, using the Bray–Curtis index (Clarke, 1993). When differences were identified, non-parametric analysis of similarity percentages (SIMPER) was employed to determine which taxonomic groups contributed most to the observed similarities and dissimilarities (Clarke and Warwick, 2001). ANOSIM and SIMPER were performed using PAST software, version 2.0 (Hammer et al., 2001). PERMANOVA was realized using PERMANOVA software, version 1.6 (Anderson, 2005). Kruskal–Wallis one-way analysis of variance on ranks was used to compare the values of photosynthetic pigments/TChl *a* ratio among depths and campaigns. Redundancy analysis (RDA) was conducted to examine the influence of environmental variables on phytoplankton (Ter Braak and Smilauer, 2002). Biomass data were transformed by applying the function log10 $(x+1)$. Forward selection was performed to determine the minimum number of factors that could explain a statistically significant proportion ($p<0.05$) of the variation in phytoplankton biomass. The selected variables were water temperature, salinity, euphotic zone (Z_{euf}) and nitrate, silicate and phosphate concentrations. The significance of these variables was assessed using Monte Carlo permutation tests with 999 unrestricted permutations.

3. Results

3.1. Oceanographic conditions

During both campaigns, South Atlantic Central Water (SACW) intruded into the continental shelf region. In the rainy season, this intrusion caused Tropical Water (TW) and SACW to mix, especially at the second depth; during the dry season, a mixture composed mainly of CW and SACW was observed at the surface, and SACW intruded into a significant portion of the continental shelf area (Foloni-Neto, 2010).

Light penetration was evaluated through the depth of euphotic zone (Z_{euf}) and was more pronounced in the ocean, especially in the rainy season. On the continental shelf, Z_{euf} varied from 6 to 60 m (mean=29 m) in the rainy period and from 18 to 48 m (mean=37 m) during the dry period. In the oceanic region, Z_{euf} varied from 30 to 75 m (mean=53 m) in the rainy season and from 18 to 60 m (mean=41 m) during the dry season.

In this study, the concentrations of all inorganic nutrients were lower in surface waters (1 m). The average orthophosphate values for the dry and rainy periods were 0.09 and 0.18 $\mu mol\ L^{-1}$ at the second depth and 0.04 and 0.15 $\mu mol\ L^{-1}$ at the surface, respectively. Nitrate was also more depleted at the surface and in the dry season, with average values of 1.18 and 1.37 $\mu mol\ L^{-1}$ at the surface, and 1.17 and 1.49 $\mu mol\ L^{-1}$ at the second depth in the dry and rainy seasons, respectively. The same patterns were observed for silicate, with an average of 1.16 and 1.57 $\mu mol\ L^{-1}$ for surface waters and 1.47 and 1.62 $\mu mol\ L^{-1}$ at the second depth in the dry and rainy seasons.

3.2. Spatial and temporal distribution of pigments

The maximum, minimum and median pigment concentrations recorded in the rainy and dry periods are presented in Tables 1 and 2, respectively. TChl *a* decreased from the coast to the oceanic region (Tables 1 and 2 and Fig. 3). On the continental shelf the obtained TChl *a* values were typical of coastal areas (maximum of

Table 1
Maximum (Max.), median (Med.) and minimum (Min.) concentrations ($\mu g\ m^{-3}$) of the main pigments found in the rainy period on the continental shelf (isobaths 25, 50 and 75 m) and in the oceanic region (isobaths 150, 400, 1000, 1900 and 3000 m), at both depths.

Pigment		Shelf 1 m (n=26)	Shelf 2nd depth (n=26)	Ocean. Reg. 1 m (n=45)	Ocean. Reg. 2nd depth (n=45)
TChl a	*Max.*	*1134*	*1856*	*343*	*496*
	Med.	*268*	*521*	*151*	*166*
	Min	*104*	*204*	*33*	*54*
Chl *a*	**Max.**	**1049**	**1856**	**276**	**383**
	Med.	**234**	**475**	**104**	**112**
	Min.	**104**	**124**	**22**	**38**
Fuco	*Max.*	*312*	*588*	*28*	*27*
	Med.	*23*	*54*	*4*	*6*
	Min.	*6*	*14*	*1*	*3*
Chl *b*	**Max.**	**90**	**336**	**21**	**89**
	Med.	**16**	**80**	**4**	**8**
	Min.	**5**	**27**	**0**	**1**
19′Hex	*Max.*	*61*	*217*	*38*	*89*
	Med.	*29*	*95*	*18*	*31*
	Min.	*17*	*31*	*6*	*12*
Zea	**Max.**	**147**	**195**	**131**	**136**
	Med.	**104**	**61**	**86**	**85**
	Min.	**39**	**23**	**29**	**39**
Chl c2	*Max.*	*104*	*191*	*22*	*40*
	Med.	*18*	*58*	*7*	*13*
	Min.	*2*	*16*	*2*	*3*
Chl *c3*	**Max.**	**43**	**165**	**19**	**47**
	Med.	**9**	**61**	**4**	**9**
	Min.	**0**	**13**	**0**	**3**
19′But	*Max.*	*15*	*161*	*17*	*50*
	Med.	*8*	*35*	*5*	*8*
	Min.	*5*	*9*	*1*	*3*
DV Chl *a*	**Max.**	**85**	**153**	**91**	**118**
	Med.	**34**	**32**	**48**	**61**
	Min.	**0**	**153**	**11**	**15**
Per	*Max.*	*69*	*147*	*14*	*10*
	Med.	*7*	*12*	*3*	*5*
	Min.	*0*	*0*	*0*	*0*
Allo	**Max.**	**25**	**87**	**10**	**6**
	Med.	**3**	**13**	**0**	**0**
	Min.	**0**	**0**	**0**	**0**
Pras	**Max.**	16	49	2	11
	Med.	2	11	0	0
	Min.	0	49	0	0
Viola	*Max.*	14	49	4	6
	Med.	4	8	1	2
	Min.	0	3	0	0
Mixo	**Max.**	18	10	16	11
	Med.	6	0	4	0
	Min.	0	0	0	0
Lut	*Max.*	13	19	0	1
	Med.	1	1	0	0
	Min.	0	0	0	0

Table 2
Maximum (Max.), median (Med.) and minimum (Min.) concentrations ($\mu g\ m^{-3}$) of the main pigments found in the dry period on the continental shelf (isobaths 25, 50 and 75 m) and in the oceanic region (isobaths 150, 400, 1000, 1900 and 3000 m), at both depths.

Pigment		Shelf 1 m (n=26)	Shelf 2nd depth (n=26)	Ocean. Reg. 1 m (n=42)	Ocean. Reg. 2nd depth (n=41)
TChl a	*Max.*	*2156*	*5507*	*2025*	*1668*
	Med.	*520*	*767*	*178*	*285*
	Min.	*117*	*184*	*57*	*88*
Chl *a*	**Max.**	**2156**	**5507**	**2025**	**1656**
	Med.	**492**	**760**	**114**	**244**
	Min.	**102**	**179**	**36**	**58**
Fuco	*Max.*	*2301*	*3277*	*195*	*1249*
	Med.	*180*	*338*	*17*	*33*
	Min.	*16*	*9*	*5*	*2*
Chl *b*	**Max.**	**401**	**468**	**135**	**156**
	Med.	**68**	**98**	**13**	**50**
	Min.	**401**	**15**	**0**	**5**
19′Hex	*Max.*	*139*	*251*	*212*	*211*
	Med.	*53*	*84*	*31*	*77*
	Min.	*20*	*21*	*11*	*22*
Zea	**Max.**	**147**	**145**	**95**	**77**
	Med.	**29**	**16**	**49**	**41**
	Min.	**11**	**0**	**14**	**5**
Chl c2	*Max.*	*464*	*971*	*150*	*317*
	Med.	*82*	*108*	*15*	*37*
	Min.	*0*	*14*	*3*	*8*
Chl *c3*	**Max.**	**312**	**558**	**110**	**289**
	Med.	**55**	**103**	**15**	**53**
	Min.	**10**	**10**	**2**	**10**
19′But	*Max.*	*56*	*92*	*63*	*109*
	Med.	*12*	*22*	*12*	*40*
	Min.	*56*	*10*	*4*	*9*
DV Chl *a*	**Max.**	**30**	**38**	**100**	**109**
	Med.	**0**	**0**	**34**	**40**
	Min.	**0**	**0**	**100**	**109**
Per	*Max.*	*28*	*44*	*18*	*16*
	Med.	*8*	*11*	*4*	*6*
	Min.	*3*	*0*	*0*	*0*
Allo	**Max.**	**102**	**60**	**543**	**41**
	Med.	**17**	**17**	**1**	**5**
	Min.	**0**	**3**	**0**	**0**
Pras	*Max.*	*102*	*103*	*31*	*33*
	Med.	*12*	*17*	*2*	*7*
	Min.	*0*	*0*	*0*	*0*
Viola	**Max.**	**57**	**60**	**21**	**22**
	Med.	**10**	**12**	**3**	**4**
	Min.	**57**	**2**	**21**	**0**
Neo	*Max.*	*59*	*39*	*19*	*61*
	Med.	*17*	*7*	*4*	*2*
	Min.	*59*	*1*	*0*	*0*
Lut	**Max.**	**27**	**70**	**6**	**4**
	Med.	**4**	**4**	**1**	**0**
	Min.	**0**	**0**	**0**	**0**

1.86 $mg\ m^{-3}$ in the rainy period and 5.51 $mg\ m^{-3}$ in the dry period). In the oceanic region the TChl *a* values were typical of oligotrophic conditions (0.03 to 0.3 $mg\ m^{-3}$ in the rainy period and 0.06 to 2.0 $mg\ m^{-3}$ in the dry period), with little variation being observed between periods. However, in the region of the shelf break (isobaths of 150 and 400 m), the biomasses observed in the northern Campos Basin (Transects H and I) were higher in the dry period (Fig. 3). Regardless of the period and bathymetry, the highest TChl *a* values were registered at the second depth.

Fuco, a pigment associated with diatoms and haptophytes, was found to be the most abundant pigment after Chl *a* (Tables 1 and 2). Higher concentrations of Fuco were registered in the dry period, especially closer to the coast. In contrast, 19′Hex and 19′But (marker pigments for haptophytes) were distributed along the bathymetric profile, and no marked temporal variation in their concentrations was apparent. The 19′But/19′Hex and 19′But/(19′But+Fuco+19′Hex) ratios varied from 0.07 to 0.25 and 0.24 to 0.52, respectively; although no temporal or spatial variations were observed, the values were usually higher for the second depth (Table 3). Chl *c3*, which is also present in haptophytes, was found at higher concentrations at the first three isobaths in the rainy period and extended to the oceanic region in the dry period. After Fuco, Chl *b* was the most abundant pigment (0–0.47 $mg\ m^{-3}$), indicating the importance of green algae in this environment (Tables 1 and 2). We also detected Lut, Neo, Viola and Pras, which are characteristic carotenoids of green algae. Zea, a marker of cyanobacteria, was evenly distributed across the Campos Basin, with slightly higher concentrations being recorded in the rainy period (0.02–0.2 $mg\ m^{-3}$). The high Zea/Chl a ratios observed (maximum ratios of 1.4 and 1.1 in the rainy and dry periods, respectively) suggested the presence of picoplanktonic cyanobacteria of the genus *Synechococcus* (Carreto et al., 2003).

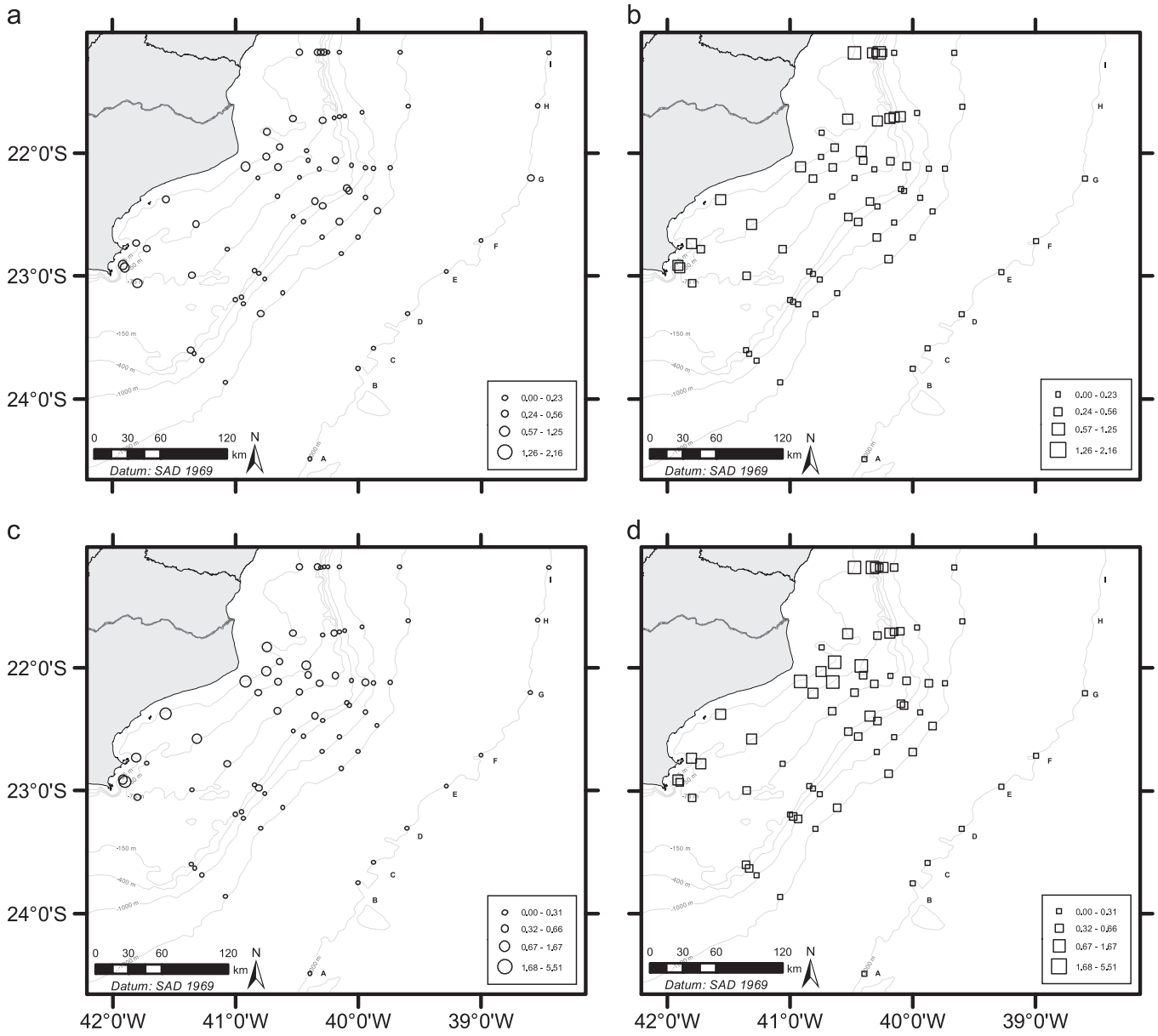

Fig. 3. Spatial distribution of TChl *a* (mg m^{-3}) in Campos Basin during the two sampling periods, at the two sampled depths. (a) Rainy period, 1 m; (b) dry period, 1 m; (c) rainy period, second depth; (d) dry period, second depth. Notice the different scales.

DV Chl *a*, an unequivocal *Prochlorococcus* pigment, was detected at significant concentrations in both periods (0–0.15 mg m^{-3}). Mixo, which is present in the filamentous cyanobacteria of the genus *Trichodesmium* (Mackey et al., 1997), was detected only in the rainy period. Per, an unequivocal dinoflagellate-associated pigment, was found at low concentrations in both studied periods, as was Allo, an unequivocal indicator of the presence of cryptophytes. However, higher concentrations of the later pigment were detected in the dry period, especially at the 150 m isobath (0.543 mg m^{-3}).

3.3. Photosynthetic pigments/TChl a ratio

The ratio between the examined Photosynthetic pigments (Per, 19′But, Fuco, 19′Hex, Pras, Allo, Chl c2, Chl c3, DV Chl b and Ch b) and TChl a was used as a proxy to evaluate photoacclimation in the phytoplankton populations (Carreto et al., 2008). This ratio was calculated for the two sampled depths on the shelf (first three isobaths) and in the oceanic region (remaining isobaths) of the Basin; the regions were defined according to the observed spatial distributions of the pigment concentrations. Photosynthetic pigments/TChl a ratios were significantly higher at the second depth on the shelf in the rainy period and in the oceanic region in the dry period (Fig. 4). The ratios were also significantly higher in the dry period than the rainy period.

3.4. CHEMTAX analysis

The presence of seven classes of phytoplankton (Bacillariophyceae, Haptophyceae, Prasinophyceae, Dinophyceae, Pelagophyceae, Cryptophyceae and Cyanobacteria) was detected in both campaigns. Two groups of prasinophytes, three groups of haptophytes and three genera of cyanobacteria (*Trichodesmium*, *Synechococcus* and *Prochlorococcus*) were distinguished. With the exception of *Trichodesmium*, which was recorded only during the rainy period campaign, all of these groups/classes were present in both campaigns.

The input matrix (Table 4) appeared to describe the environment well because in both periods and at both depths, the output ratios (Tables 5 and 6) generally did not differ dramatically from

the initial input values. In the following cases, differences between the output and input ratios should be noted: in the rainy period, the Fuco/Chl a ratio for diatoms was lower in the shelf region, and the Per/Chl *a* ratio for dinoflagellates on the shelf was higher for the second depth. For pelagophytes, during the rainy period, 19′But/Chl a increased, while Fuco/Chl a decreased with depth. The ratios obtained for type 8 haptophytes were stable, except for on the shelf in the dry period, where the 19′Hex/Chl a values were found to be much lower for the second depth. The Chl c3/Chl a ratios were stable, except for those of type 8 haptophytes on the shelf in the dry period. The Zea/Chl a ratio obtained for *Synechococcus* was quite stable, showing a tendency towards somewhat lower values in the dry period, while Zea/Chl *a* for *Prochlorococcus* displayed little variation across the sampling periods and depths (0.32–0.44). Beyond the shelf break, Pras/Chl a decreased while Chl b/Chl a decreased for prasinophytes (type 1).

3.5. Spatial and temporal distribution of phytoplankton groups

No spatial patterns in the distribution of phytoplankton with respect to the latitudinal profile were identified. Statistical analyses (PERMANOVA) revealed significant differences only in the shelf region, for transect H, which differed from transects A and C in the southern Campos Basin in the rainy period ($p < 0.05$) and from all transects except A in the dry period ($p < 0.05$). SIMPER analysis showed that the difference observed in the dry period was due to a greater prasinophyte and haptophyte contribution and a low cryptophyte and diatom biomass (data not shown).

Distinct spatial patterns were observed along the bathymetric profile for the phytoplankton groups. The diatom biomass was high at the 25 and 50 m isobaths and then declined dramatically with the distance from the shore (Fig. 5). The biomass of nanoplanktonic flagellate organisms (prasinophytes, haptophytes and cryptophytes) generally decreased with the distance from the shore (Figs. 5–7). The spatial distribution pattern observed for pelagophytes (eukaryotic picoplankton) was distinct: pelagophyte biomass increased toward the 400 m isobath and declined in the oceanic region (Fig. 7). Among the identified cyanobacteria (Fig. 8), *Trichodesmium* was recorded only in the rainy period and was widely distributed in both the shelf and oceanic regions, displaying higher biomasses at the surface. *Synechococcus* was also present in both periods, but no spatial distribution pattern was found for this genus at either sampling depth. During the rainy period campaign, the biomass of the picoplanktonic *Prochlorococcus* increased from coastal areas toward the 400 m isobath and was equally distributed in the oceanic region. However, during the dry period, a distinct gradient was apparent, with *Prochlorococcus* biomass increasing from the 150 m isobath to the oceanic region.

With respect to the vertical distribution, ANOSIM revealed a significant difference ($p < 0.05$) between the phytoplankton assemblages at the two depths in both the shelf and oceanic regions. SIMPER analysis showed that the vertical patterns observed were related to both the sampling period (rainy or dry) and the region (shelf or oceanic). Diatoms were the group that was most responsible for the dissimilarity observed in the shelf region, where the highest diatom biomass was measured, at the second depth (Fig. 5). In the oceanic region, cyanobacteria and haptophytes showed greater variability

Table 3
Mean and standard deviations of the 19′But/(19′But + Fuco + 19′Hex) and 19′But/19′Hex ratios in the continental shelf and oceanic regions in the rainy and dry periods at the two sampled depths.

Ratio	Rainy period		Dry period	
	Continental shelf ($n=27$)	Oceanic region ($n=45$)	Continental shelf ($n=27$)	Oceanic region ($n=42$)
19′But/(19′But + Fuco + 19′Hex)				
1 m	0.13 ± 0.06	0.16 ± 0.02	0.07 ± 0.06	0.18 ± 0.06
2nd Depth	0.20 ± 0.12	0.19 ± 0.03	0.10 ± 0.09	0.25 ± 0.09
19′But/19′Hex				
1 m	0.28 ± 0.07	0.25 ± 0.05	0.24 ± 0.06	0.37 ± 0.10
2nd Depth	0.50 ± 0.20	0.30 ± 0.07	0.35 ± 0.18	0.52 ± 0.16

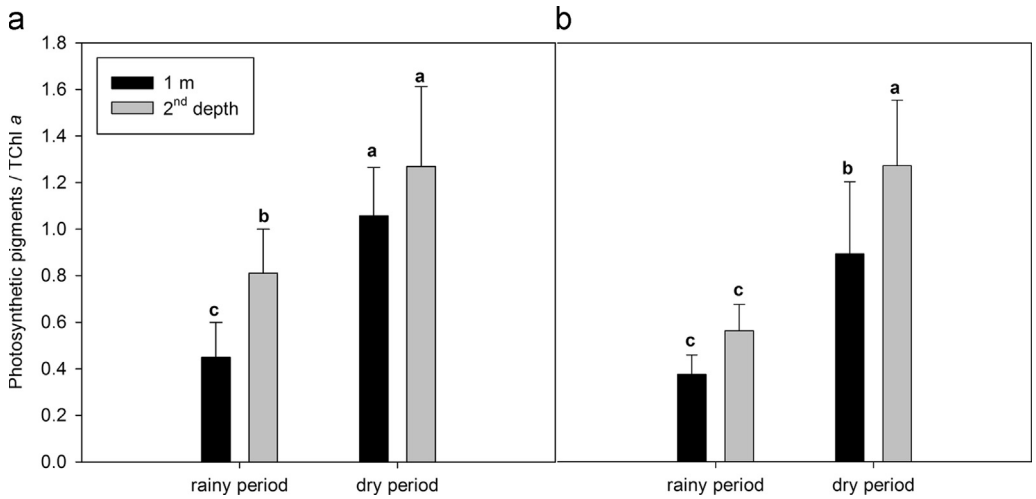

Fig. 4. Photosynthetic pigments/TChl *a* ratios at the two sampled depths, in the (a) shelf region (25 to 75 m isobaths); (b) oceanic region (150 to 3000 m isobaths) during the rainy and dry periods. Different symbols ((a)–(c)) denote statistically significant differences ($p < 0.05$).

Table 4
CHEMTAX Input ratio-matrix (pigment/chlorophyll *a*).

Class/Pigment	per	19but	fuco	19hex	neox	pras	violax	allo	lut	zea	Mixo	chl_b	chlc2	chlc3
Pras1					0.113	0.458	0.000		0.018	0.079		0.679		
Pras2					0.079	0.000	0.138		0.049	0.043		0.532		
Dinofl	0.411												0.099	
Crypt								0.261					0.057	
Hapt6		0.021	0.100	1.060									0.230	0.240
Hapt7		0.062	0.360	0.720									0.110	0.090
Hapt8		0.220	0.480	0.450									0.100	0.310
Syn										1.245				
Tric										0.048	0.034			
Proc										0.327				
Pel		0.510	0.732										0.397	0.174
Diat			0.863										0.208	

Table 5
CHEMTAX output matrices for the rainy period. (Means of the 6 matrices that generated the lowest residuals. The mean coefficient of variation of the pigment ratios in the matrices ranged from 13 to 20%).

	Per	19but	fuco	19hex	neox	pras	violax	allo	lut	zea	Mixo	chl_b	chlc2	chlc3
Shelf—1 m														
Pras1					0.113	0.454			0.020	0.080		0.662		
Pras2					0.074	0	0.147		0.041	0.040		0.544		
Dinofl	0.391												0.097	
Crypt								0.272					0.056	
Hapt6		0.021	0.095	0.772									0.217	0.253
Hapt7		0.053	0.305	0.979									0.112	0.082
Hapt8		0.210	0.487	0.448									0.090	0.380
Syn										1.689				
Tric										0.095	0.091			
Proc										0.381				
Pel		0.588	0.555										0.391	0.167
Diat			0.578										0.169	
Shelf—2nd depth														
Pras1					0.112	0.428			0.021	0.070		0.725		
Pras2					0.082	0	0.112		0.026	0.047		0.614		
Dinofl	0.648												0.114	
Crypt								0.252					0.058	
Hapt6		0.021	0.101	0.969									0.197	0.254
Hapt7		0.058	0.361	0.764									0.110	0.090
Hapt8		0.182	0.301	0.456									0.112	0.409
Syn										1.533				
Tric										0.042	0.033			
Proc										0.369				
Pel		0.881	0.397										0.353	0.190
Diat			0.684										0.200	
Oceanic region—1 m														
Pras1					0.124	0.436			0.017	0.078		0.706		
Pras2					0.078		0.139		0.047	0.043		0.600		
Dinofl	0.372												0.096	
Crypt								0.237					0.061	
Hapt6		0.021	0.068	1.182									0.286	0.205
Hapt7		0.067	0.336	0.687									0.113	0.085
Hapt8		0.181	0.413	0.470									0.107	0.360
Syn										1.656				
Tric										0.087	0.102			
Proc										0.325				
Pel		0.643	0.354										0.349	0.156
Diat			0.781										0.222	
Oceanic region—2nd depth														
Pras1					0.125	0.248			0.017	0.076		0.909		
Pras2					0.063	0	0.137		0.013	0.044		0.731		
Dinofl	0.360												0.101	
Crypt								0.252					0.061	
Hapt6		0.019	0.054	1.056									0.267	0.264
Hapt7		0.065	0.339	0.874									0.101	0.088
Hapt8		0.209	0.469	0.411									0.103	0.303
Syn										1.562				
Tric										0.113	0.076			
Proc										0.443				
Pel		0.874	0.325										0.378	0.170
Diat			0.827										0.207	

Table 6
CHEMTAX output matrices for the dry period. (Means of the 6 matrices which generated the lowest residuals. The mean coefficient of variation of the pigment ratios in the matrices ranged from 13 to 20%).

	per	19but	fuco	19hex	neox	pras	violax	allo	lut	zea	chl_b	chlc2	chlc3
Shelf—1 m													
Pras1					0.090	0.481			0.016	0.081	0.782		
Pras2					0.146	0	0.151		0.056	0.049	0.597		
Dinofl												0.086	
	0.351												
Crypt								0.244				0.063	
Hapt6		0.023	0.101	1.010								0.209	0.292
Hapt7		0.065	0.404	0.706								0.107	0.092
Hapt8		0.129	0.517	0.437								0.095	0.602
Syn										1.313			
Proc										0.370			
Pel		0.619	0.696									0.384	0.179
Diat			1.009									0.254	
Shelf—2nd depth													
Pras1					0.115	0.480			0.017	0.089	0.642		
Pras2					0.065	0	0.157		0.042	0.040	0.832		
Dinofl	0.365											0.102	
Crypt								0.280				0.076	
Hapt6		0.026	0.119	1.151								0.255	0.264
Hapt7		0.056	0.331	0.593								0.114	0.092
Hapt8		0.037	0.589	0.142								0.113	0.709
Syn										1.611			
Proc										0.285			
Pel		0.703	0.778									0.416	0.208
Diat			0.868									0.231	
Oceanic region—1 m													
Pras1					0.136	0.324			0.018	0.083	0.906		
Pras2					0.190		0.143		0.040	0.034	0.542		
Dinofl												0.095	
	0.360												
Crypt								0.275				0.081	
Hapt6		0.024	0.089	1.075								0.229	0.273
Hapt7		0.069	0.367	0.683								0.116	0.088
Hapt8		0.202	0.509	0.412								0.090	0.359
Syn										1.370			
Proc										0.362			
Pel		0.559	0.610									0.396	0.179
Diat			0.762									0.203	
Oceanic region—2nd depth													
Pras1					0.078	0.227			0.016	0.082	1.159		
Pras2					0.435		0.032		0.039	0.076	0.255		
Dinofl	0.389											0.090	
Crypt								0.239				0.057	
Hapt6			0.093	1.240								0.227	0.262
	0.021												
Hapt7			0.357	0.772								0.105	0.089
	0.061												
Hapt8			0.404	0.465								0.100	0.313
	0.245												
Syn										1.200			
Proc										0.304			
Pel			0.554									0.353	0.198
	0.617												
Diat			0.890									0.213	

between depths (Figs. 6 and 8). In the rainy period, *Trichodesmium* preferred the layers nearer the water's surface, whereas the Prochlorococcus and haptophyte biomasses were higher at the second depth. In contrast, during the dry period, prasinophytes were evenly distributed between the sampling depths, while the cryptophyte biomass was greater at 1 m (Figs. 5 and 7). *Synechococcus* biomass was higher at the surface (1 m).

3.6. Structure of phytoplankton assemblages

Because no statistically significant differences between transects were identified, the median of the values obtained for all transects for a particular isobath was considered a good representation of the phytoplankton assemblage at that isobath (Fig. 9). In the rainy season, different assemblage structures were observed for the two sampling depths. At 1 m (Fig. 9a), the region closest to the coast (25 and 50 m isobaths) was distinct from the remaining isobaths (ANOSIM, $p < 0.05$). This region was characterized by equal contributions from diatoms, cyanobacteria and haptophytes (approximately 24% from each), with 16% of the biomass being composed of prasinophytes. From the 75 to the 3000 m isobath, there was no significant difference observed between the plankton assemblages: micro- and picoplanktonic cyanobacteria contributed 70% of the total biomass on average (29% *Prochlorococcus*, 22% *Synechococcus* and 19% *Trichodesmium*). At the second depth (Fig. 9b), two regions could be discerned: one on the shelf, from the 25 to the 75 m isobath, and another beginning

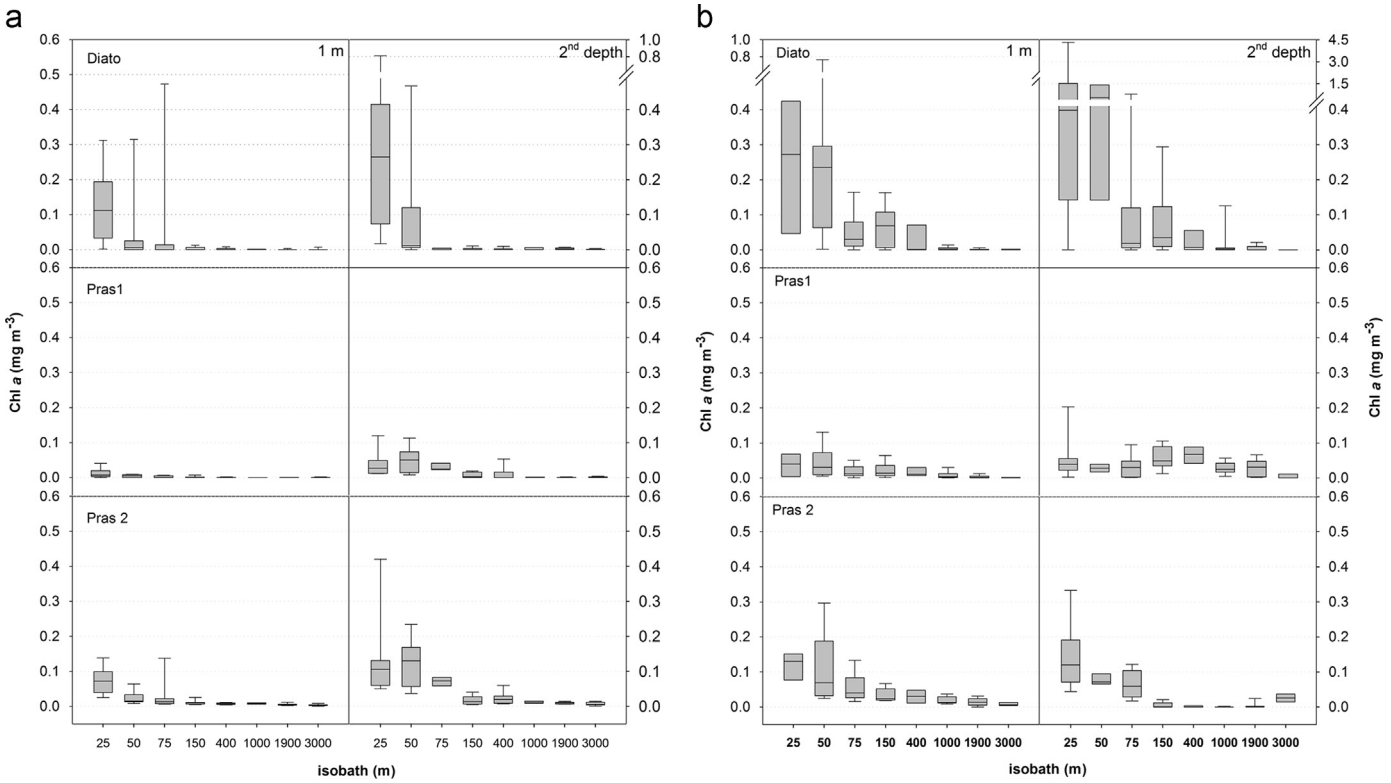

Fig. 5. Biomass variation (expressed in mg m^{-3} Chl *a*) for diatoms and prasinophytes (with prasinoxanthin: Pras1, and without prasinoxanthin: Pras2) in samples collected at 1 m and at second depth on different isobaths in the (a) rainy and (b) dry period collection campaigns. The lines within the boxes are medians; the boxes correspond to 25–75% of the data and the bars to 90%.

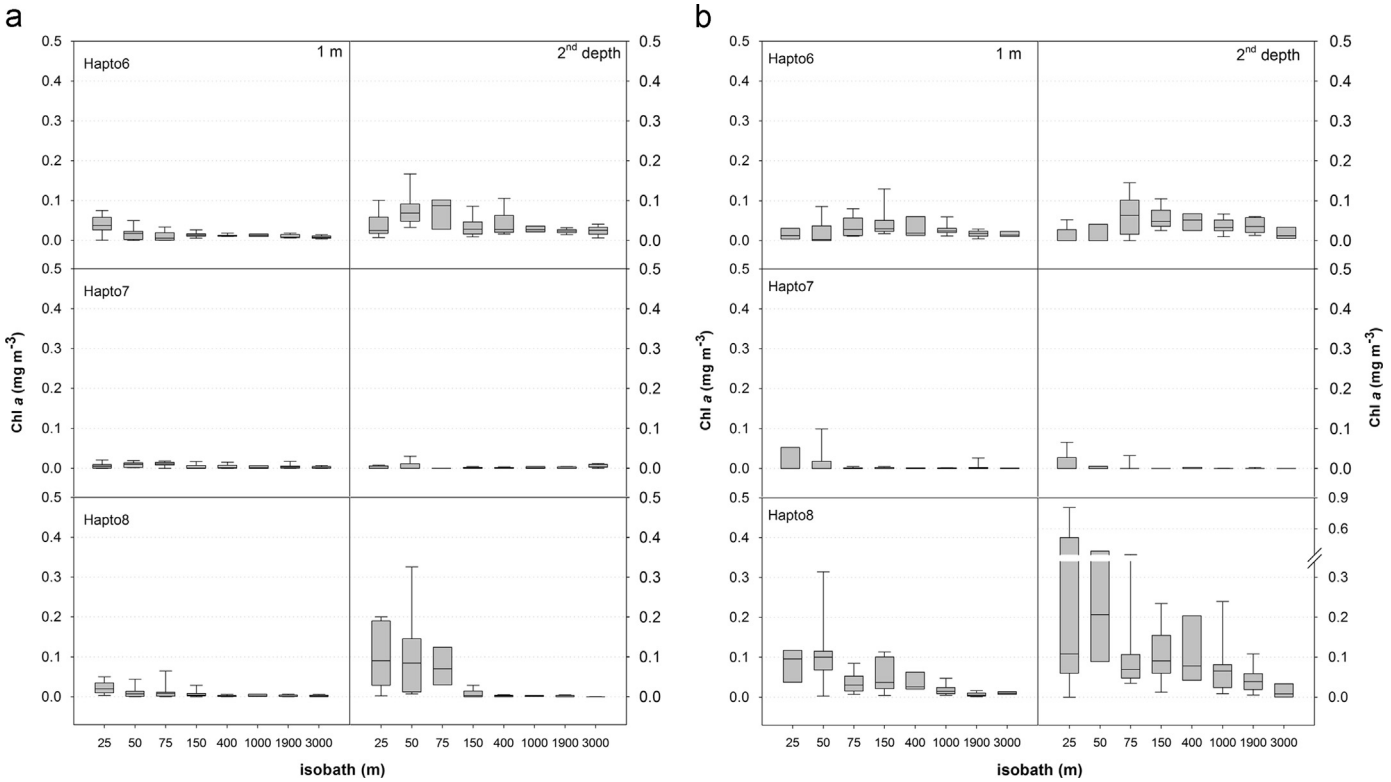

Fig. 6. Biomass variation (expressed in mg m^{-3} Chl *a*) for haptophytes (types 6–8) in samples collected at 1 m and at second depth on different isobaths in the (a) rainy and (b) dry period collection campaigns. The lines within the boxes are medians; the boxes correspond to 25–75% of the data and the bars to 90%.

on the shelf at the 150 m isobath and extending throughout the oceanic region (ANOSIM, $p < 0.05$). Diatoms predominated (35% of biomass) at the second depth near the coast (25 m isobath), but in this case, the high relative importance of haptophytes and prasinophytes (15–40% and 18–34%, respectively) extended into the 75 m isobath. From the 150 to the 3000 m isobath, picoplanktonic cyanobacteria

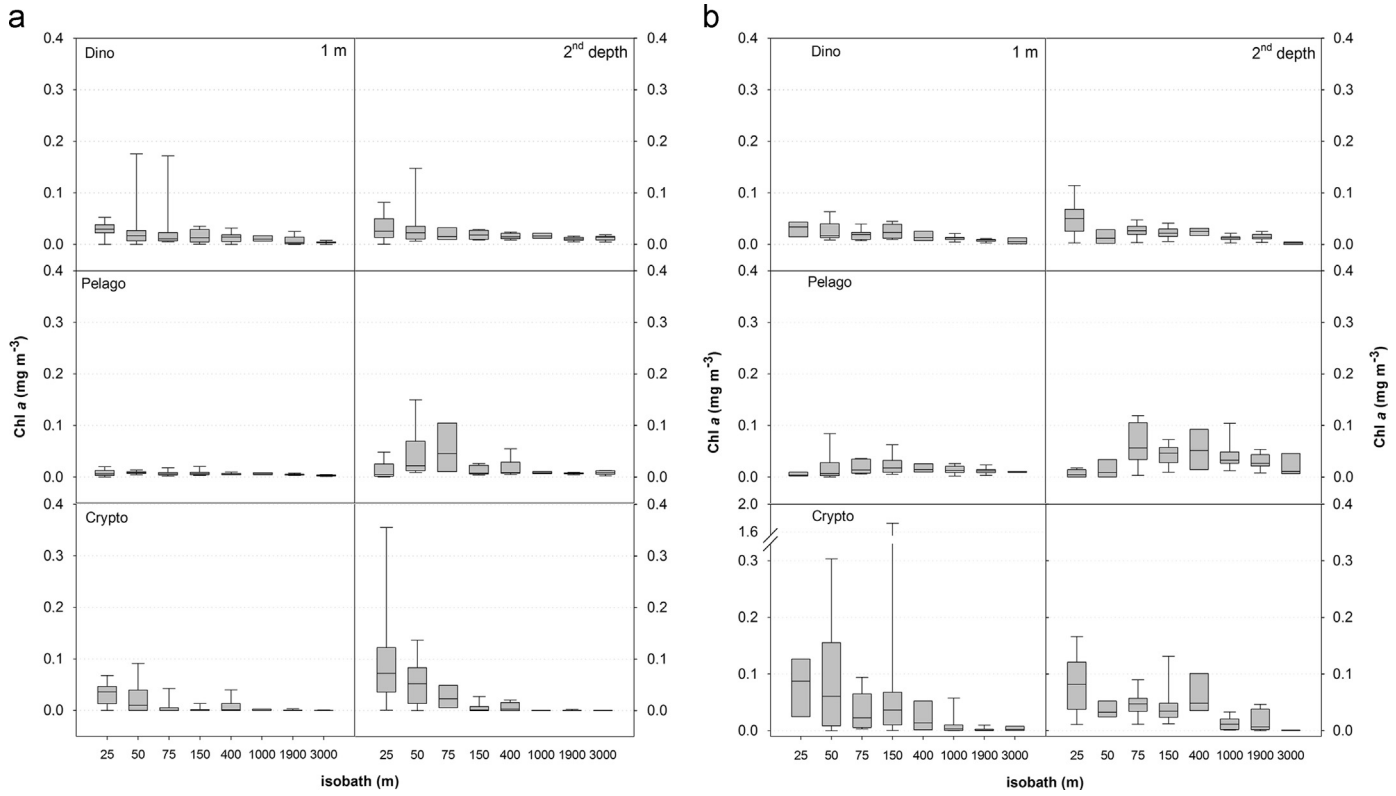

Fig. 7. Biomass variation (expressed in mg m^{-3} Chl *a*) for dinoflagellates, pelagophytes and cryptophytes in samples collected at 1 m and at second depth on different isobaths in the (a) rainy and (b) dry period collection campaigns. The lines within the boxes are medians; the boxes correspond to 25–75% of the data and the bars to 90%.

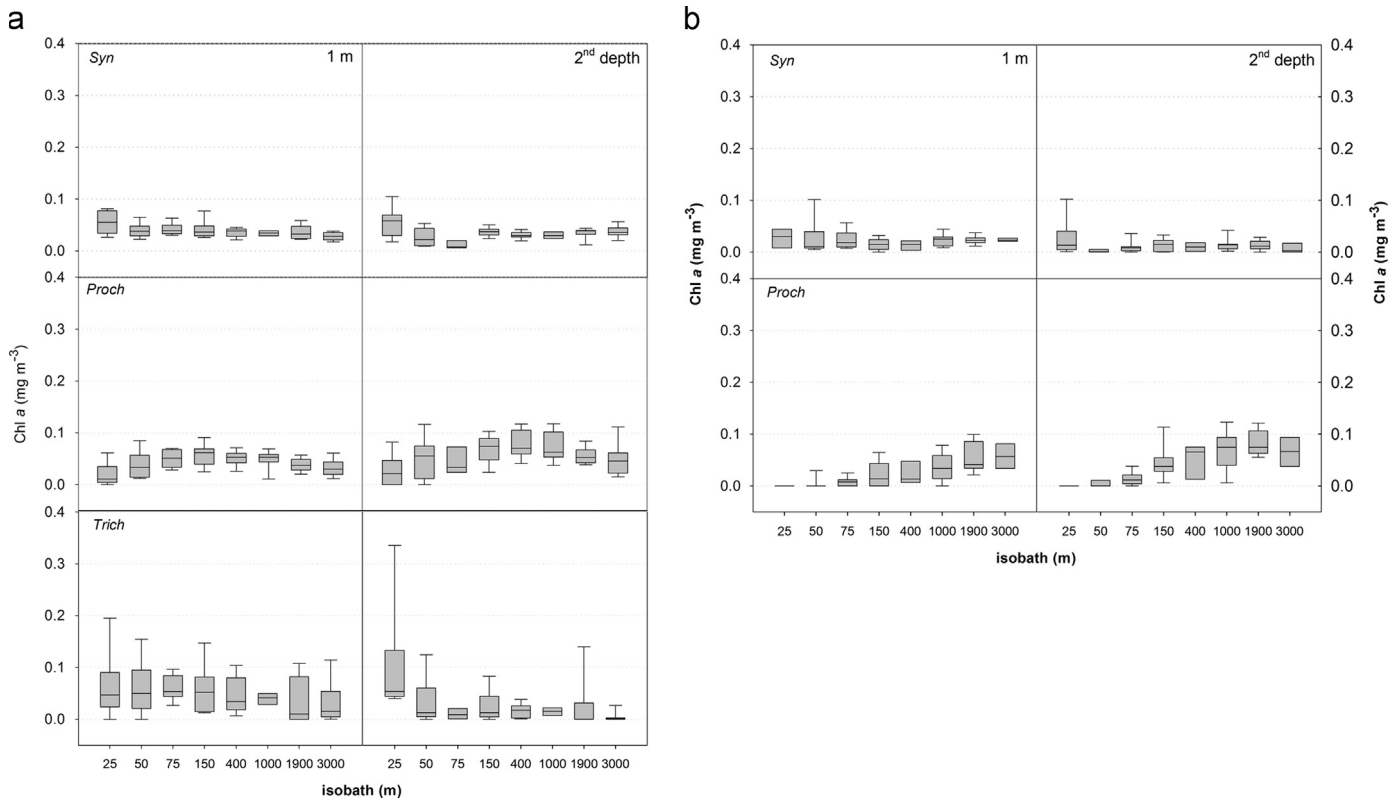

Fig. 8. Biomass variation (expressed in mg m^{-3} Chl *a*) for *Synechococcus*, *Prochlorococcus*, and *Trichodesmium* in samples collected at 1 m and at second depth on different isobaths in the (a) rainy and (b) dry period collection campaigns (*Trichodesmium* was not detected in the dry period). The lines within the boxes are medians; the boxes correspond to 25–75% of the data and the bars to 90%.

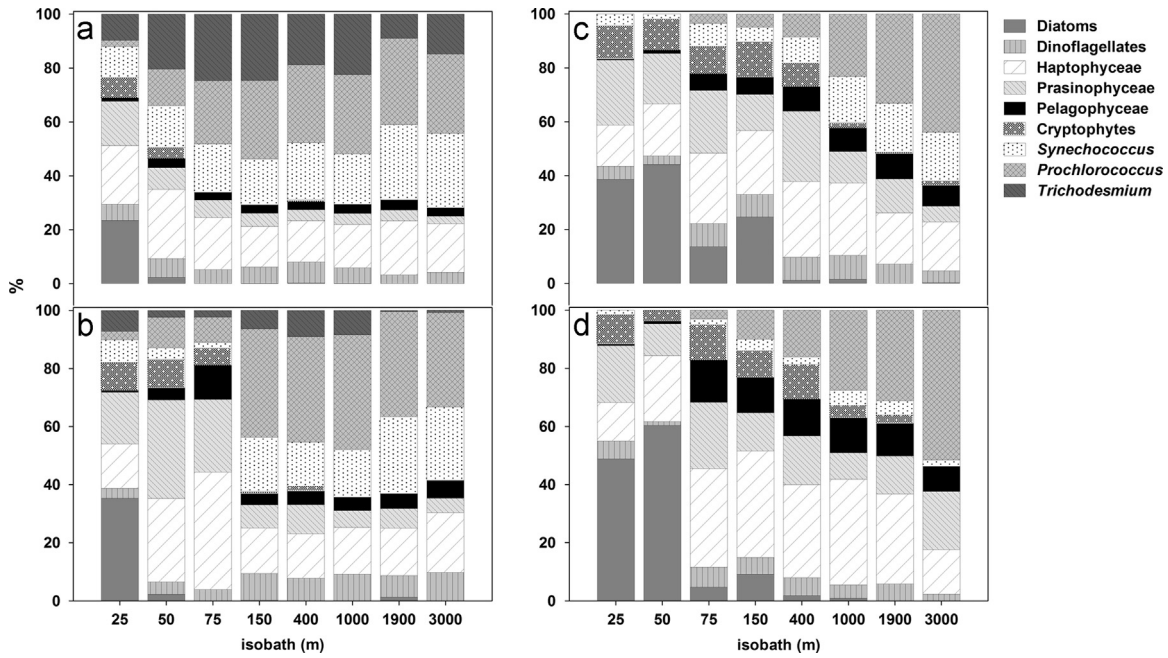

Fig. 9. Proportional contributions of algal groups to samples collected during the rainy period (left panel: (a) 1 m, (b) second depth) and dry period (right panel: (c) 1 m, (d) second depth). Values are medians for isobaths.

(36% *Prochlorococcus* and 20% *Synechococcus*) dominated; the contribution of *Trichodesmium* was low relative to the surface layer; and haptophytes accounted for approximately 17% of the plankton biomass.

In the dry period (Fig. 9c and d), the coastal region (25 and 50 m isobaths) was still distinct due to the large contributions of diatoms and nanoflagellates to total biomass (ANOSIM, $p < 0.05$). Moving away from the coast, from the 150 to the 3000 m isobath, there was a gradual change in the assemblage structure from dominance of nanoplanktonic groups (haptophytes, prasinophytes and cryptophytes) to picoplanktonic cyanobacteria (mainly *Prochlorococcus*). At 1 m, the planktonic biomass in the more coastal isobaths (25 and 50 m) was, on average, composed of 41% diatoms, 17% haptophytes, 21% prasinophytes and 12% cryptophytes; thereafter, a gradient from 26% haptophytes, 23% prasinophytes and 13% diatoms at the 75 m isobath to 44% *Prochlorococcus*, 18% *Synechococcus* and 18% haptophytes at the 3000 m isobath was observed. For the 25 and 50 m isobaths, the second depth showed a similar composition. However, the proportional contribution of *Synechococcus* decreased, while that of nanoflagellates and picoplanktonic pelagophytes was higher than for the surface waters. At the 3000 m isobath, dominance of *Prochlorococcus* was observed (51%), with important contributions from prasinophytes (20%) and haptophytes (15%).

3.7. Correlation between phytoplankton groups and environmental variables

A Monte Carlo test of *F*-ratios indicated that the six environmental variables considered contributed significantly to explaining the spatial and temporal distributions of the phytoplankton groups (salinity: $F=59.34$, $p<0.01$; water temperature: $F=32.49$, $p<0.01$; silicate concentration: $F=3.70$, $p<0.01$; nitrate concentration: $F=2.58$, $p<0.05$; phosphate concentration: $F=3.39$, $p<0.01$; depth of the euphotic zone: $F=1.97$, $p<0.05$). The first two ordination axes from the RDA explained 94% ($F=18.89$, $p<0.01$) of the spatial/temporal distribution of phytoplankton groups, with 69% being explained by the first canonical axis and 25% by the second (Fig. 10). A temporal pattern defined by higher salinities and temperatures in the rainy period and higher nutrient concentrations in the dry period was detected. A spatial gradient associated with the bathymetric profile was also apparent, with higher concentrations of nutrients, particularly silicate, being found in samples from the shelf region and higher salinities and greater euphotic zone depths being observed within the oceanic region.

The identified phytoplankton groups displayed the following patterns. Cyanobacteria predominated in rainy season samples, and *Prochlorococcus* was associated with oceanic waters. Moreover, diatoms and nanoflagellates (Haptophyceae, Prasinophyceae and Cryptophyceae) were associated with higher nutrient availability in the dry season. In addition, there was a distinct association of picoplanktonic eukaryotes (Pelagophyceae) with the oceanic region in the dry period.

4. Discussion

4.1. Pigment data and definition of the taxonomic groups

The use of two parallel HPLC methods served as a form of quality control, as the two quantification methods were compared to detect inconsistencies. This procedure allowed the detection and quantification of 21 pigments.

The positive correlation ($r=0.540$, $p<0.01$, $n=52$ for log-transformed data) of Mixo with *Trichodesmium* biomass (data obtained via microscopy, Tenenbaum, per. comm.) supported its inclusion as a marker for this taxon. Although they were not included in the CHEMTAX input ratios, the pigments monovinyl-Chl c3 and Chl *c2*-monogalactosyldiacylglyceride ester, from *Chrysochromulina* (Seoane et al., 2009), which occur in haptophyte types 6 and 7 (sensu Zapata et al., 2004), were detected in some samples in small amounts, confirming the presence of these two taxonomic groups.

The 19′But/19′Hex and 19′But/(19′But+Fuco+19′Hex) ratios can aid in the interpretation of pigment data and in recognition of the taxonomic groups of haptophytes present. The calculated 19′But/19′Hex and 19′But/(Fuco+9′But+19′Hex) ratios (Table 3) were compared with those found by Seoane et al. (2009) for haptophytes, after transforming the molar ratios reported by these

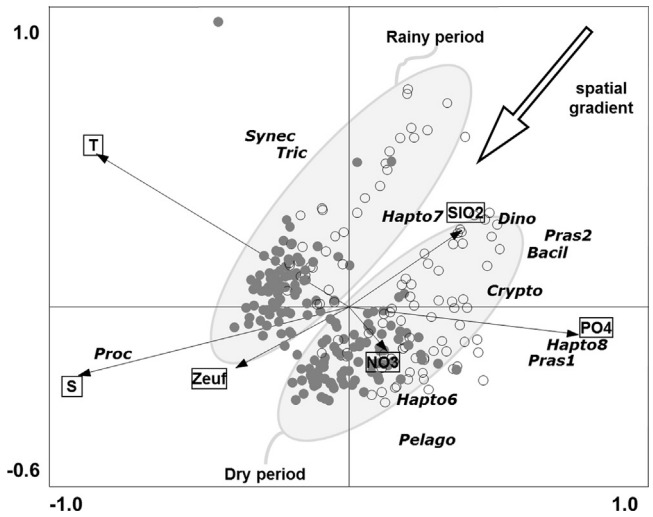

Fig. 10. RDA ordination diagram with vectors for environmental variables (T—water temperature, S—salinity, Z_{euf}—euphotic zone, NO3—nitrate, PO4—phosphate, SIO2—silicate) and phytoplankton groups (Proc—*Prochlorococcus*, Synec—*Synechococcus*, Tric—*Trichodesmium*, Hapto6/Hapto7/Hapto8—haptophytes types 6–8, Pras1/Pras2—prasinophytes with and without prasinoxanthin, Dino—dinoflagellates, Bacil—diatoms, Crypto—cryptophytes, Pelago—pelagophytes). White dots represent samples from the continental shelf and gray dots represent samples from the oceanic region. The arrow indicates the spatial gradient from the shelf to the oceanic region.

authors into mass ratios. With the exception of the ratios calculated for the continental shelf in the dry period, the average 19′But/(Fuco+9′But+19′Hex) values obtained in this study were higher than the maximum of 0.12 reported in the literature (Laza-Martinez et al., 2007; Seoane et al., 2009) for haptophyte types 1, 2, 3, 6, 7 and 8 (sensu Zapata et al., 2004). Moreover, all of the mean values of the 19′But/19′Hex ratio calculated here were greater than 0.23, which was the maximum value obtained by Seoane et al. (2009) for haptophytes. The pigment 19′But is present in multiple types of haptophytes as well as in picoplanktonic pelagophytes (Dimier et al., 2009). Thus, haptophytes type 8 and pelagophytes, which display a high 19′But content, were included in the present study.

The detection of Pras indicated the presence of prasinophytes of type I (sensu Latasa and Scharek, 2004) in the Campos Basin. Studies conducted using cultures of type I prasinophytes indicate that the Pras/Chl b ratio can vary from 0.17 to 0.77 (Schlüter et al., 2003). Lower ratios indicate the presence of type II prasinophytes and/or Chlorophyceae. Because ratios below 0.17 were observed in the Campos Basin, it can be assumed that type II prasinophytes or Chlorophyceae are additional sources of Chl b in this area. However, the low Lut/Chl b ratios observed (0.01 to 0.13 in the rainy period and 0.00 to 0.20 in the dry period) argue against the presence of Chlorophyceae, which exhibit Lut/Chl b ratios higher than 0.30 (Schlüter et al., 2003).

4.2. CHEMTAX analysis

Due to the large number of stations sampled (72), it was possible to perform CHEMTAX analyses separately for the shelf and oceanic regions and for the two depths in each sampling period. After running CHEMTAX with 60 different input matrices and taking the mean of the six best results, as suggested by Wright et al. (2009), we did not consider it necessary to run CHEMTAX successively for each of the six best output matrices, as some authors have performed (De Souza et al., 2012; Schlüter et al., 2011). We observed that the output ratios of the main pigments of the dominant taxonomic groups generally tended to stabilize with the reduction of residuals, which was the main factor involved in the stabilization of taxonomic group biomass.

The observed decrease in the 19′Hex/Chl a output ratio observed at the second depth for type 8 haptophytes on the shelf during the dry period could be explained by a change in the species composition of this group. For diatoms, a higher Fuco/Chl a content was observed in the dry period, which may reflect different physiological states of the cells (Schlüter et al., 2011) or the presence of other fucoxanthin-containing taxonomic groups, such as type 1–5 haptophytes (which do not contain 19′Hex and 19′But) or dinoflagellate species, such as *Gymnodinium* sp., which contain fucoxanthin and related pigments, but no peridinin (Zapata et al., 1998; Carreto et al., 2001).

4.3. Spatio-temporal distribution of the phytoplanktonic groups

The phytoplankton biomass estimated by TChl a showed high variability in the Campos Basin (Tables 1 and 2, Fig. 3). The observed TChl *a* values in waters over the shelf were typical of Brazilian coastal regions (Gonzalez-Rodriguez et al., 1992; Knoppers et al., 1999), while the concentrations recorded in the oceanic region were characteristic of oligotrophic waters found in systems such as the Brazil Current (Gonzalez-Silvera et al., 2004; Carreto et al., 2008). The observed gradient in TChl *a* concentration was coincident with changes in phytoplankton composition (Fig. 9). Gradients of TChl *a* are known to be associated with shifts in composition of phytoplankton assemblages from micro- and nanoplankton predominance in eutrophic and mesotrophic waters, respectively, to nearly equal pico- and nanoplankton contributions in oligotrophic waters (Uitz et al., 2006).

Over the shelf, the intrusion of SACW (Foloni-Neto, 2010) was responsible for the high nutrient concentrations observed. These intrusions of nutrient rich waters can promote algal growth on photic zone. Based on the significant correlations found with silicate ($r=0.44$, $p<0.01$) and phosphate ($r=0.65$, $p<0.01$) concentrations in the rainy period and phosphate concentrations ($r=0.33$, $p<0.01$) in the dry period, the observed variability in the spatial (bathymetric profile) and temporal (dry and rainy season) biomass patterns may be partly related to the availability of nutrients, particularly phosphorus and silica (Fig. 10).

Although this result is unexpected, since nitrogen is considered the main driver of phytoplankton biomass in marine waters (e.g., Howarth and Marino, 2006; Carlsson et al., 2012), phosphorus limitation is also common in marine systems (Downing et al., 1999; Elser et al., 2007). Furthermore, although no significant correlations between phytoplankton biomass and nitrate were found, low dissolved inorganic nitrogen values were also observed (<7 μmol L^{-1}), which could be indicative of a potential nitrogen limitation (Reynolds, 2006). Co-limitation by nitrogen and phosphorus is also reported in many studies (Arrigo, 2005; Zohary et al., 2005).

The vertical distribution of inorganic nutrients showed patterns which are typical of permanently stratified tropical waters, with higher values found in the continental shelf. Nutrient concentrations observed at the second depth were always higher than those obtained at surface waters, and were consistent with contribution/intrusions of SACW to this depth. Phosphorus limitation was potentially more severe in surface waters with an average N/P ratio of 32 (1 m) vs. 20 (2nd depth). Potential P limitation was more intense during the rainy season, as P levels were the lowest. The vertical distribution pattern of some phytoplankton groups, showing greater biomass at the second depth, was related to a higher nutrient availability (Figs. 5–8).

However, light availability can also be an important driver in the Campos Basin region. Although most of the time the 2nd depth was in the euphotic zone, in many cases the samples were collected at depths greater than Zeu. This was the case during

the rainy period at the shelf and for almost all the samples collected in the oceanic region during the dry period (data not shown). Physiological adaptations in terms of pigment composition allow populations to have greater access to nutrients, without suffering light limitation. The increase in the Photosynthetic Pigments/TChl a ratio observed at the second depth indicates this type of photoacclimation response (Carreto et al., 2008) and was observed for the entire Campos Basin region. The disparity was more distinct in the rainy season, when large differences between the surface (Photosynthetic Pigments/TChl $a=0.45$) and the second depth (Photosynthetic Pigments/TChl $a=0.8$) were recorded. This reflects the period of greatest vertical stratification of the water column.

Diatoms, nanoflagellates and picoplanktonic cyanobacteria dominated the phytoplankton assemblages with respect to total biomass. Diatoms were more prevalent in the coastal region (25–50 m isobaths), especially in periods of increased nutrient availability. In the Abrolhos region (northeast coast of Brazil), HPLC/CHEMTAX analysis also detected important contributions of diatoms to plankton assemblages near the coast, which was not observed in the oceanic region (Knoppers et al., 1999).

Microplanktonic diatoms are associated with conditions of high turbulence and nutrient availability (Margalef, 1978; Falkowski, 1980). Many diatom species can be considered R-strategists (disturbance tolerant, or ruderal), presenting a high Surface/Volume ratio that affords them the ability to harvest light energy under strong mixing conditions, but with high nutrient concentrations (Reynolds, 1997; Alves-de-Souza et al., 2008). The generally high maximum uptake rates observed in diatoms may be advantageous under conditions of high or fluctuating nutrient availability (Turpin, 1988; Grover, 1991; Litchman et al., 2007).

Planktonic nanoflagellates, especially haptophytes and prasinophytes, were found to be important in the Campos Basin region. Phytoplanktonic assemblages were characterized by the dominance of these organisms in regions that extend from areas near the coast to the shelf break (150–400 m isobaths; Fig. 9). The importance of prasinophytes in the Brazil Current was also noted by Carreto et al. (2008), particularly at the base of the euphotic zone. In the present work, pigment analysis was very important in quantifying the contributions of these groups. Pras 2 (violaxanthin-containing prasinophytes), detected primarily on the shelf in the Campos Basin, has been previously reported in coastal areas (Ruivo et al., 2011). The prasinoxanthin-containing prasinophytes (Egeland et al., 1995) (Pras1 in this work) found both on the shelf and in the oceanic region, are picoplanktonic species that appear to be the most abundant picoeukaryotes in coastal waters (Meakin and Wyman, 2011) and can be ubiquitous in oceanic regions around the world (Worden and Not, 2008).

The three types of haptophytes detected in the present study have also been reported in the Brazil Current (Carreto et al., 2008). The type 6 haptophytes include *Emiliania huxleyi*, which is the most abundant and cosmopolitan coccolithophore species, frequently constituting ~50% of the coccolithophore flora (McIntyre and Bé, 1967; Okada and Honjo, 1973). Type 8 includes *Phaeocystis*, which displays a worldwide distribution and is an important component of the haptophycean assemblage (Thomsen et al., 1994; Schoemann et al., 2005). Moreover, *Chrysochromulina* (type 7) and *Phaeocystis* and *Imantonia* (type 8) were found on the Brazilian coast at the maritime front of Lagoa dos Patos (Bergesch et al., 2008). In the Campos Basin, type 6 haptophytes were found primarily in the outer shelf region, while type 8 haptophytes showed a preference for the inner shelf. The biomass of each group was higher at the second depth. Carreto et al. (2008) also observed greater concentrations of haptophytes types 6 and 8 at a depth of 30 m than at the surface in the shelf break area of the Rio de la Plata front. The change in species composition observed for the type 8 group in the shelf at the second depth in the dry period was most likely related to the incidence of SACW at the second depth, while a mixture of TW with SACW was present at 1 m.

Carreto et al. (2008) and Mendes et al. (2011) attributed the presence of nanoflagellate species with rapid growth rates (*r*-selected species) in the shelf break region to circulation patterns that produce internal waves resulting in nutrient inputs. Both haptophytes and prasinophytes can be considered C-strategists (competitors, opportunistic colonizers), which are expected to dominate in waters with high nutrient concentrations and light availability (Reynolds, 1997). According to a classification proposed for phytoplankton by Sommer (1984), prasinophytes appear to exhibit a 'velocity-adapted' strategy, as they exhibit high maximum growth rates (Litchman et al., 2007). In fact, the greatest abundance of haptophytes and prasinophytes was observed during the dry period, when the SACW reached the shelf, bringing nutrients. In addition to being small organisms with rapid growth rates, haptophytes exhibit low half-saturation constants for nutrient uptake (Litchman et al., 2007), which may optimize nutrient acquisition under low nutrient conditions (Turpin, 1988; Grover, 1991). Haptophytes are well adapted not only to low nutrient conditions but also to the high irradiance levels that are often associated with such conditions (Iglesias-Rodriguez et al., 2002). This 'affinity' strategy (Sommer, 1984) was evident during the dry period, when the haptophyte contributions to planktonic assemblages in the oceanic region of the Campos Basin were significant, particularly at the second depth.

The oceanic region of the Campos Basin was characterized by dominance of picoplanktonic cyanobacteria (*Prochlorococcus* and *Synechococcus*). Similar results were obtained through pigment/CHEMTAX analysis in the warm, highly stratified, nutrient-poor oceanic waters of the Brazil Current at the Maritime Front of the Rio de la Plata (Carreto et al., 2003, 2008). *Synechococcus* is found in nearly all oceanic surface waters (Partensky et al., 1999), whereas the distribution of *Prochlorococcus* is restricted to strongly stratified oligotrophic waters (Bouman et al., 2006) in tropical or subtropical regions. Moreover, *Prochlorococcus* is often present at a low abundance or is absent from coastal waters where *Synechococcus* thrives (Partensky et al., 1999; Gibb et al., 2000).

Our results showed that *Prochlorococcus* was present almost exclusively in oceanic waters (in both the dry and rainy periods), or in the shelf area during periods of low nutrient concentrations and strong stratification (rainy period). In contrast, *Synechococcus* was widely distributed in both the shelf and oceanic regions (Figs. 8 and 9). These two genera exhibit distinct ecological niches; their requirements for key environmental factors (light and nitrogen) are determined by their light-harvesting antennae and their intracellular nitrogen requirements, which are lower in *Prochlorococcus* (Ting et al., 2002). Niche differentiation in these cyanobacteria can be linked to the variation in light quality between coastal and oceanic waters. *Synechococcus* is equipped for growth in green light, which predominates in coastal waters, whereas *Prochlorococcus* is particularly efficient at absorbing the blue wavelengths of light that penetrate to depths of 100–200 m in the ocean (Moore et al., 1998; Partensky et al., 1999). In open ocean regions where *Prochlorococcus* and *Synechococcus* co-occur, *Prochlorococcus* has generally been found to extend deeper in the water column than *Synechococcus* (Partensky et al., 1999). Photoadapted phytoplankton populations were previously found in the Brazil Current at the sea front of the River de la Plata by Carreto et al. (2008). These authors also highlighted the presence of two distinct populations of *Prochlorococcus*, one growing at the surface, reflecting an ecotype adapted to high light intensities (low DV Chl b/DV Chl a ratios), and one growing in deeper layers, representing an ecotype with photoadapted ratio values >2 (Ting et al., 2002; Carreto et al., 2008). The data obtained in the Campos Basin also

suggest that the identified *Prochlorococcus* populations exhibit physiological responses that indicate photoadaptation, with higher DV Chl b/DV Chl a ratio values being found at the second depth. However, we were unable to distinguish the presence of different ecotypes because the obtained DV Chl b/DV Chl a ratios were always below 1 (Moore et al., 1995; Ting et al., 2002).

In addition to the picoplanktonic species discussed above, species of the genus *Trichodesmium* were also important in the Campos Basin. This genus was recorded only during the rainy period and was widely distributed in both the shelf and oceanic regions, with higher biomasses being recorded at the surface. The significant contribution of *Trichodesmium* to the cyanobacterial biomass was consistent with previous reports describing the occurrence of this genus throughout oligotrophic tropical and subtropical oceans (Capone et al., 1997; Bergman et al., 2013). The fact that this genus was not registered in the dry period may be related to the lower water temperatures recorded during this period (19–24 °C). *Trichodesmium* abundance is roughly limited to waters warmer than 20 °C, and the temperature tolerance of these species with respect to growth ranges from 20 to 34 °C (Breitbarth et al., 2007; Chappell and Webb, 2010).

5. Conclusion

The pigment analysis using HPLC in conjunction with CHEMTAX software performed here made it possible to characterize the composition and structure of phytoplankton assemblages in the Campos Basin. SACW seasonal intrusions over the continental shelf not only influence the stratification of the water column, but particularly influence the availability of nutrients in the continental shelf region. This hydrological regime was crucial to the dynamics of the phytoplankton community. On the continental shelf, diatoms (R-strategists) were more prevalent in the coastal region in periods of increased availability of nutrients, associated with increased conditions of turbulence. Nanoplanktonic groups (C-strategists-haptophytes and prasinophytes) predominated on the outer shelf and the shelf break, associated with high nutrient concentrations and availability of light. The variation in light quality between coastal and oceanic waters was probably responsible for the distributions of *Prochlorococcus* and *Synechococcus* observed. *Prochlorococcus* was present almost exclusively in oceanic waters (in both dry and rainy periods) or in the shelf area during periods of low nutrient concentrations and strong stratification (rainy period). In contrast, *Synechococcus* was widely distributed in both the shelf and oceanic regions.

Acknowledgements

We thank Drs. Denise Tenenbaum and Silvia Nascimento for microplankton information. We are thankful for the constructive criticism of three anonymous reviewers, which helped to improve the manuscript.

References

Alves-de-Souza, C., Gonzalez, M.T., Iriarte, J.L., 2008. Functional groups in marine phytoplankton assemblages dominated by diatoms in fjords of southern Chile. J. Plankton Res. 30, 1233–1243.
Anderson, M.J., 2001. A new method for non-parametric multivariate analysis of variance. Austral Ecol. 26, 32–46.
Anderson, M.J., 2005. PERMANOVA: A FORTRAN Computer Program for Permutational Variance. Department of Statistics, University of Auckland, New Zealand
Arrigo, K.R., 2005. Marine microorganisms and global nutrient cycles. Nature 437, 349–355.
Bergesch, M., Odebrecht, C., Moestrup, O., 2008. Nanoflagellates from coastal waters of southern Brazil (32°S). Bot. Mar. 51, 35–50.
Bergman, B., Sandh, G., Lin, S., Larsson, J., Carpenter, E.J., 2013. *Trichodesmium*—a widespread marine cyanobacterium with unusual nitrogen fixation properties. FEMS Microbiol. Rev. 37, 286–302.
Bouman, H., Ulloa, O., Scanlan, D.J., Zwirglmaier, K., Li, W.K.W., Platt, T., Stuart, V., Barlow, R., Leth, O., Clementson, L., Lutz, V., Fukasawa, M., Watanabe, S., Sathyendranath, S., 2006. Oceanographic basis of the global surface distribution of *Prochlorococcus* ecotypes. Science 312, 918–921.
Brandini, F.P., 1988. Hydrography, Phytoplankton Biomass and Photosynthesis in Shelf and Oceanic Waters Off Southeastern Brazil During Autumn (May/June 1983). Bolm. Institute of Oceanography, University of Sao Paulo 36, 63–72.
Breitbarth, E., Oschlies, A., LaRoche, J., 2007. Physiological constraints on the global distribution of *Trichodesmium*—effect of temperature on diazotrophy. Biogeosciences 4, 53–61.
Brotas, V., Plante-Cuny, M., 2003. The use of HPLC pigment analysis to study microphytobenthos communities. Acta Oecol. 24, 109–115.
Capone, D.G., Zehr, J.P., Paerl, H.W., Bergman, B., Carpenter, E.J., 1997. *Trichodesmium*, a globally significant marine cyanobacterium. Science 276, 1221–1229.
Carlsson, P., Granéli, E., Granéli, W., Rodriguez, E.G., Carvalho, W.F., Brutemark, A., Lindehoff, E., 2012. Bacterial and phytoplankton nutrient limitation in tropical marine waters, and a coastal lake in Brazil. J. Exp. Mar. Biol. Ecol. 418–419, 37–45.
Carreto, J.I., Seguel, M., Montoya, N.G., Clément, A., Carignan, M.O., 2001. Pigment profile of the ichthyotoxic dinoflagellate *Gymnodinium* sp. from a massive bloom in southern Chile. J. Plankton Res. 23, 1171–1175.
Carreto, J.I., Montoya, N.G., Benavides, H.R., Guerrero, R., Carignan, M.O., 2003. Characterization of spring phytoplankton communities in the Río de La Plata maritime front using pigments signatures and cell microscopy. Mar. Biol. 143, 1013–1023.
Carreto, J.I., Montoya, N.G., Akselman, R., Carignan, M.O., Silva, R.I., Cucchi-Colleoni, D.A., 2008. Algal pigment patterns and phytoplankton assemblages in different water masses of the Rio de la Plata maritime front. Cont. Shelf Res. 28, 1589–1606.
Chappell, P.D., Webb, E.A., 2010. A molecular assessment of the iron stress response in the two phylogenetic clades of *Trichodesmium*. Environ. Microbiol. 12, 13–27.
Clarke, K.R., 1993. Non-parametric multivariate analysis of changes in community structure. Aust. J. Ecol. 18, 117–143.
Clarke, K.R., Warwick, R.M., 2001. Change in Marine Communities: An Approach to Statistical Analysis and Interpretation. 5Primer-E Ltd, Plymouth Marine Laboratory, UK.
Cole, G.A., 1994. Textbook of Limnology. Waveland Press Inc., Illinois.
De Souza, M.S., Mendes, C.R.B., Garcia, V.M.T., Pollery, R., Brotas, V., 2012. Phytoplankton community during a coccolithophorid bloom in the Patagonian Shelf: microscopic and high performance liquid chromatography pigment analyses. J. Mar. Biol. Assoc. U. K. 92, 13–27.
Dimier, C., Brunet, C., Geider, R., Raven, J., 2009. Growth and photoregulation dynamics of the picoeukaryote *Pelagomonas calceolata* in fluctuating light. Limnol. Oceanogr. 54, 823–836.
Downing, J.A., Osenberg, C.W., Sarnelle, O., 1999. Meta-analysis of marine nutrient-enrichment experiments: variation in the magnitude of nutrient limitation. Ecology 80, 1157–1167.
Ediger, D., Soydemir, N., Kideys, A.E., 2006. Estimation of phytoplankton biomass using HPLC pigment analysis in the southwestren Black SeaDeep Sea Res. Part II 53, 1911–1922.
Egeland, E.S., Eikrem, W., Throndsen, J., Wilhelm, C., Zapata, M., Liaaen-Jensen, S., 1995. Carotenoids from further prasinophytes. Biochem. Syst. Ecol. 23, 747–755.
Elser, J.J., Bracken, M.E.S., Cleland, E.E., Gruner, D.S., Harpole, E.S., Hillebrand, H., Ngai, J.T., Seabloom, E.W., Shurin, J.B., Smith, J.E., 2007. Global analysis of nitrogen and phosphorus limitation of primary producers in freshwater, marine and terrestrial ecosystems. Ecol. Lett. 10, 1135–1142.
Falkowski, P.G., 1980. Light-shade adaptation in marine phytoplankton. In: Falkowski, P.G. (Ed.), Primary Productivity in the Sea. Plenum Press, New York (99–19).
Fernandes, L.F., Brandini, F.P., 2004. Diatom associations in shelf waters off Parana State, Southern Brazil: annual variation in relation to environmental factors. Braz. J. Oceanogr. 52, 19–34.
Foloni-Neto, H., 2010. As massas d´água da Bacia de Campos. University of São Paulo p. 120 (RJ. MSc. Thesis. Oceanographic Institute).
Gianesella-Galvão, S.M.F., Costa, M.P.F., Kutner, M.B.B., 1995. Bloom of *Oscilllatoria* (*Trichodesmium*) erythraea (Ehr.) Kütz. in Coastal Waters of the Southwest Atlantic. Special Issue Institute of Oceanography, University of Sao Paulo 11, 133–140.
Gibb, S.W., Barlow, R.G., Cummings, D.G., Rees, N.W., Trees, C.C., Holligan, P., Suggett, D., 2000. Surface phytoplankton pigment distributions in the Atlantic Ocean: an assessment of basin scale variability between 50 degrees N and 50 degrees S. Prog. Oceanogr. 45, 339–368.
Gieskes, W.W.C., Kraay, G.W., Nontji, A., Setiapermana, D., Sutomo, 1988. Monsonal alternation of a mixed and layered structure in the phytoplankton of the euphotic zone of the Banda Sea (Indonesia): a mathematical analysis of algal pigments fingerprints. J. Sea Res. 22, 123–137.
Gonçalves-Araujo, R., De-Souza, M.S., Mendes, C.R.B., Tavano, V.M., Pollery, C., Garcia, C.A.E., 2012. Brazil-Malvinas confluence: effects of environmental variability on phytoplankton community structure. J. Plankton Res. 34, 399–415.
Gonzalez-Rodriguez, E., Valentin, J.L.V., Andre, D.L., Jacob, S.A., 1992. Upwelling and downwelling at Cabo Frio (Brazil)—comparison of biomass and primary production responses. J. Plankton Res. 17, 289–306.
Gonzalez-Silvera, A., Santamaria-del-Angel, E., Garcia, V.M.T., Garcia, C.A.E., Millán-Nuñez, R., Muller-Karger, F., 2004. Biogeographical regions of the tropical and subtropical Atlantic Ocean off South America: classification based on pigment (CZCS) and chlorophyll-a (SeaWiFS) variability. Cont. Shelf Res. 24, 983–1000.
Grasshoff, K., Ehrhardt, M., K. Kremling, K., 1999. Methods of Seawater Analysis, third ed. Verlag Chemie, Weinheim.

Grob, C., Ulloa, O., Claustre, H., Huot, Y., Alarcón, G., Marie, D., 2007. Contribution of picoplankton to the total particulate organic carbon concentration in the eastern South Pacific. Biogeosciences 4, 837–852.

Grover, J., 1991. Dynamics of competition among microalgae in variable environments: experimental tests of alternative modelOikos 62, 231–243 (Retrieved from)⟨http://www.jstor.org/stable/10.2307/3545269⟩.

Guenther, M., Gonzalez-Rodriguez, E., Carvalho, W.F., Rezende, C.E., Mugrabe, G., Valentin, J.L., 2008. Plankton trophic structure and particulate organic carbon production during a coastal downwelling–upwelling cycle. Mar. Ecol. Prog. Ser. 363, 109–119.

Hammer, Ø., Harper, D.A.T., Ryan, P.D., 2001. PAST: paleontological statistics software package for education and data analysis. Palaeontol. Electron. 4 (art.4), 9.

Howarth, R., Marino, R., 2006. Nitrogen as the limiting nutrient for eutrophication in coastal marine ecosystems: evolving views over three decades. Limnol. Oceanogr. 51, 364–376.

Iglesias-Rodriguez, M.D., Brown, C.W., Doney, S.C., Kleypas, J.A., Kolber, D., Kolber, Z., Hayes, P.K., Fakowski, P.G., 2002. Representing key phytoplankton functional groups in ocean carbon cycle models: coccolithophorids. Global Biogeochem. Cycles 16 (art), 1100.

Knoppers, B., Meyerhofer, M., Marone, E., Dutz, J., Lopes, R., Leipe, T., De Camargo, R., 1999. Compartments of the pelagic system and material exchange at the Abrolhos Bank coral reefs, Brazil. Arch. Fish. Mar. Res. 47, 285–306.

Latasa, M., Scharek, R., 2004. Pigments suites and taxonomic groups in prasinophyceae. J. Phycol. 40, 1149–1155.

Laza-Martinez, A., Seoane, S., Zapata, M., Orive, E., 2007. Phytoplankton pigment patterns in a temperate estuary: from unialgal cultures to natural assemblages. J. Plankton Res. 29, 913–929.

Letelier, R.M., Bidigare, R.R., Hebel, D.V., Ondrusek, M., Winn, C.D., Karl, D.M., 1993. Temporal variability of phytoplankton community structure based on pigment analysis. Limnol. Oceanogr. 38, 1420–1437.

Litchman, E., Klausmeier, C., Schofield, O.M., Falkowski, P.G., 2007. The role of functional traits and trade-offs in structuring phytoplankton communities: scaling from cellular to ecosystem level. Ecol. Lett. 10, 1170–1181.

Mackey, M.D., Higgins, H.W., Mackey, D.J., Wright, S.W., 1997. CHEMTAX User's Manual: A Program for Estimating Class Abundances from Chemical Markers—Applications to HPLC Measurements of Phytoplankton Pigments. Hobart, Australia p. 47 (CSIRO Mar. Laboratories Report 229).

Margalef, R., 1978. Life-forms of phytoplankton as survival alternative in an unstable environment. Oceanolog. Acta 1, 493–509.

Marinho, M., Rodrigues, S.V., 2003. Phytoplankton of an eutrophic reservoir: comparison of biomass estimated from counts with chlorophyll-a biomass from HPLC measurements. Hydrobiologia 505, 77–88.

McIntyre, A., Bé, A., 1967. Modern coccolithophoridae of the Atlantic Ocean-I. Placoliths and cyrtoliths. Deep Sea Res. 14, 561–597.

Meakin, N.G., Wyman, M., 2011. Rapid shifts in picoeukaryote community structure in response to ocean acidification. ISME J. 5, 1397–1405.

Mendes, C.R., Sá, C., Vitorino, J., Borges, C., Tavano-Garcia, V.M., Brotas, V., 2011. Spatial distribution of phytoplankton assemblages in the Nazaré submarine canyon region (Portugal): HPLC-CHEMTAX approach. J. Mar. Syst. 87, 90–101.

Miller, J.C., Miller, J.N., 1988. Statistics for Analytical Chemistry, second ed. Ellis Horwood, Chichester.

Moore, L.R., Goerike, R., Chisholm, S.W., 1995. Comparative physiology of *Synechococcus* and *Prochlorococcus*: influence of light and temperature on growth, pigment, fluorescence and absorptive properties. Mar. Ecol. Prog. Ser. 116, 259–275.

Moore, L.R., Rocap, G., Chisholm, S.W., 1998. Physiology and molecular phylogeny of coexisting *Prochlorococcus* ecotypes. Nature 393, 464–467.

Obayashi, Y., Tanoue, E., Suzuki, K., Handa, N., Nojiri, Y., Wong, C.S., 2001. Spatial and temporal variabilities of phytoplankton community structure in the northern North Pacific as determined by phytoplankton pigments. Deep Sea Res. Part I 48, 439–469.

Okada, H., Honjo, S., 1973. The distribution of oceanic coccolithophorids in the Pacific. Deep Sea Res. 20, 355–374.

Palóczy, A., Silveira, I.C.A., Castro, B.M., Calado, L., 2013. Coastal upwelling off Cape São Tomé (22°S, Brazil): the supporting role of deep ocean processes. Cont. Shelf Res. , http://dx.doi.org/10.1016/j.csr.2013.09.005.

Partensky, F., Hess, W.R., Vaulot, D., 1999. *Prochlorococcus*, a key marine photosynthetic prokaryote. Microbiol. Mol. Biol. Rev. 63, 106–127.

Reynolds, C.S., 1997. Vegetation Processes in the Pelagic: A Model for Ecosystem Theory. Ecology Institute, Oldendorf/Luhe.

Reynolds, C.S., 2006. The Ecology of Phytoplankton. Cambridge University Press, Cambridge.

Ruivo, M., Amorim, A., Cartaxana, P., 2011. Effects of growth phase and irradiance on phytoplankton pigment ratios: implications for chemotaxonomy in coastal waters. J. Plankton Res. 33, 1012–1022.

Sato, S., Paranaguá, M.N., Eskinazi, E., 1963. On the Mechanism of the Red Tide of Trichodesmiun in Recife Northeastern Brazil, with Some Considerations of the Relation to the Human Disease "Tamandaré Fever". Trab. Oceanogr. Univ. Fed. PE 5, 7–49.

Schlüter, L., Mohlenberg, F., Havskum, H., Larsen, S., 2000. The use of phytoplankton pigments for identifying and quantifying phytoplankton groups in coastal areas: testing the influence of light and nutrients on pigment/chlorophyll a ratios. Mar. Ecol. Prog. Ser. 149, 49–63.

Schlüter, L., Mohlenberg, F., 2003. Detecting presence of phytoplankton groups with non-specific pigment signatures. J. Appl. Phycol. 15, 465–476.

Schlüter, L., Henriksen, P., Nielsen, T.G., Jakobsen, H.H., 2011. Phytoplankton composition and biomass across the southern Indian Ocean. Deep Sea Res. Part I 58, 546–556.

Schoemann, V., Becquevort, S., Stefels, J., Rousseau, V., Lancelot, C., 2005. *Phaeocystis* blooms in the global ocean and their controlling mechanisms: a review. J. Sea Res. 53, 43–66.

Seoane, S., Garmendia, M., Revilla, M., Borja, A., Franco, J., Emma-Orive, E., Valencia, V., 2011. Phytoplankton pigments and epifluorescence microscopy as tools for ecological status assessment in coastal and estuarine waters, within the Water Framework Directive. Mar. Pollut. Bull. 62, 1484–1497.

Seoane, S., Zapata, M., Orive, E., 2009. Growth rates and pigment patterns of haptophytes isolated from estuarine waters. J. Sea Res. 62, 286–294.

Shi, X.L., Marie, D., Jardillier, L., Scanlan, D.J., Vaulot, D., 2009. Groups without cultured representatives dominate eukaryotic picophytoplankton in the oligotrophic South East Pacific Ocean. PLoS One 4 (10), e7657, http://dx.doi.org/10.1371/journal.pone.0007657.

Simon, N., Cras, A.L., Foulon, E., Lemée, R., 2009. Diversity and evolution of marine phytoplankton. C.R. Biol. 332, 159–170.

Sommer, U., 1984. The paradox of the plankton: fluctuations of phosphorus availability maintain diversity of phytoplankton in flow-through cultures. Limnol. Oceanogr. 29, 633–636.

Suzuki, M.S., Paranhos, R., Rezende, C.E., Pinto, F.N., Gobo, A.R., Pedrosa, P., (in press). Hidroquímica, carbono orgânico e nutrientes dissolvidos e particulados na Bacia de Campos. In: Carreira, R.S., Falcão, A.P.C. (Eds.), Caracterização Ambiental Regional da Bacia de Campos, Atlântico Sudoeste: Química Ambiental. (Série Habitats). Elsevier, Rio de Janeiro.

Tenenbaum, D.R., Gomes, E.A.T., Guimarães, G.P., 2006. Microorganismos Planctônicos: Pico, Nano e Micro. In: Valentin, J.L. (Ed.), Características hidrobiológicas da região central da Zona Econômica Exclusiva brasileira (Salvador, BA, ao Cabo de São Tomé, RJ). Ideal Gráfica e Editora, Brasília, pp. 83–124.

Tenenbaum, D.R., Nascimento, S.M., Vianna, S., Fragoso, G., Hatherly, M., Moraes, R., in press. A Estrutura Espacial e Temporal da Comunidade do Microplâncton na Bacia de Campos. In: Moreira, D.L., Falcão, A.P.C. (Eds.), Caracterização Ambiental Regional da Bacia de Campos, Atlântico Sudoeste: Ambiente Pelágico. (Série Habitats). Elsevier, Rio de Janeiro.

Ter Braak, C.J.F., Smilauer, P., 2002. CANOCO Reference Manual and CanoDraw for Windows User's guide: Software for Canonical Community Ordination (version 4.5). Microcomputer Power, Ithaca.

Thomsen, H.A., Buck, K.R., Chavez, F.P., 1994. Haptophytes as components of marine phytoplankton. In: Green, J., Leadbeater, B. (Eds.), The Haptophyte algae. Oxford University Press, Oxford, pp. 187–208.

Ting, C.S., Rocap, G., King, J., Chisholm, S.W., 2002. Cyanobacterial photosynthesis in the oceans: the origins and significance of divergent light-harvesting strategies. Trends Microbiol. 10, 134–142.

Turpin, D.H., 1988. Physiological mechanisms in phytoplankton resource competition. In: Sandgren, C.D. (Ed.), Growth and Reproductive Strategies of Freshwater Phytoplankton. Cambridge University Press, Cambridge, pp. 316–368.

Uitz, J., Claustre, H., Morel, A., Hooker, S., 2006. Vertical distribution of phytoplankton communities in open ocean: an assessment based on surface chlorophyll. J. Geophys. Res. 111, C08005, http://dx.doi.org/10.1029/2005JC003207.

Van Heukelem, L., Thomas, C.S., 2001. Computer-assisted high performance liquid chromatography method development with applications to the isolation and analysis of phytoplankton pigments. J. Chromatogr. A 910, 31–49.

Vaulot, D., Eikrem, W., Viprey, M., Moreau, H., 2008. The diversity of eukaryotic marine picophytoplankton. FEMS Microbiol. Rev. 32, 795–820.

Worden, A.Z., Not, F., 2008. Ecology and Diversity of Picoeukariotes. In: Kirchman, D.L., D.L. (Eds.), Microbial Ecology of the Oceans. Wiley, Hoboken, NJ, pp. 159–205.

Wright, S.W., Jeffrey, S.W., 1997. High Resolution HPLC System for chlorophylls and carotenoids of marine phytoplankton. In: Jeffrey, S.W., Mantoura, R.F.C., Wright, S.W. (Eds.), Phytoplankton Pigments in Oceanography—Guidelines to Modern Methods. Unesco Publishing, pp. 327–341.

Wright, S.W., Ishikawa, A., Marchant, H.J., Davidson, A.T., Van den Enden, R.L., Nash, G.V., 2009. Composition and significance of picoplankton in Antarctic waters. Polar Biol. 32, 797–808.

Wright, S.W., Van den Enden, R.L., Pearce, I., Davidson, A.T., Scott, F.J., Westwood, K.J., 2010. Phytoplankton community structure and stocks in the southern Ocean (30–80°E) determined by CHEMTAX analysis of HPLC pigmens signatures. Deep Sea Res. Part II 57, 758–778.

Zapata, M., Freire, J., Garrido, J.L., 1998. Pigment composition of several harmful algae as determined by HPLC using pyridine-containing mobile phases and a polymeric octadecylsilica column. In: Reguera, B., Blanco, J., Fernandez, M.L., Wyatt, T. (Eds.), Harmful Algae. Xunta de Galicia and Intergovernmental Oceanographic Commission of UNESCO, pp. 304–307.

Zapata, M., Jeffrey, S.W., Wright, S.W., Rodríguez, F., Garrido, J.L., Clementson, L., 2004. Photosynthetic pigments in 37 species (65 strains) of Haptophyta: implications for oceanography and chemotaxonomy. Mar. Ecol. Prog. Ser. 270, 83–102.

Zohary, T., Herut, B., Krom, M.D., Mantoura, R.F.C., Pitta, P., Psarra, S., Rassoulzadegan, F., Stambler, N., Tanaka, T., Thingstad, F., Woodward, E.M.S., 2005. P-limited bacteria but N and P co-limited phytoplankton in the Eastern Mediterranean—a microcosm experiment. Deep Sea Res. Part II 52, 3011–3023.